Widely targeted metabolite profiling of mango stem apex during floral induction by compond of mepiquat chloride, prohexadione-calcium and uniconazole

Fei Liang [1,2], **Wentian Xu** [1], **Hongxia Wu** [1], **Bing Zheng** [1], **Qingzhi Liang** [1], **Yingzhi Li** [Corresp., 2], **Songbiao Wang** [Corresp. 1]

[1] Key Laboratory of Tropical Fruit Biology of Ministry of Agriculture, South Subtropical Crops Research Institute, Chinese Academy of Tropical Agricultural Sciences, Zhanjiang, China

[2] Binhai Agricultural College of Guangdong Ocean University, 524088, Zhanjiang, China

Corresponding Authors: Yingzhi Li, Songbiao Wang
Email address: liyz@gdou.edu.cn, wsbcjy@163.com

Background. Insufficient low temperatures in winter and soil residues caused by paclobutrazol (PBZ) application pose a considerable challenge for mango floral induction (FI). Gibberellin inhibitors SPD (compound of mepiquat chloride, prohexadione-calcium and uniconazole) had a significant influence on enhancing the flowering rate and yield of mango for two consecutive years (2020-2021). Researchers have indicated that FI is regulated at the metabolic level; however, little is known about the metabolic changes during FI in response to SPD treatment. **Methods.** Here, ultra-performance liquid chromatography-electrospray ionization-tandem mass spectrometry (UPLC-ESI-MS/MS)-based widely targeted metabolomic analysis was carried out to assess the metabolic differences in the mango stem apex during different stage of mango FI (30, 80, 100 days after SPD/water treatment). **Results.** A total of 582 compounds were annotated and 372 metabolites showed two-fold differences in abundance (Variable Importance in Projection,VIP ≥ 1 and Fold change, FC≥2 or≤0.5) between buds at 30, 80, 100 days after SPD/water treatment or between buds under different treatment. Lipids, phenolic acids, amino acids, carbohydrates, and vitamins were among metabolites showing significant differences over time after SPD treatment. Here, 18 out of 20 lipids, including the lysophosphatidylethanolamine (12, LPE), lysophosphatidylcholine (7, LPC), and free fatty acids (1, FA), were significantly upregulated from 80 to 100 days after SPD treatment comared to water treatment. Meanwhile, the dormancy release of mango buds from 80 to 100 days after SPD treatment was accompanied by the accumulation of proline, ascorbic acid, carbohydrates, and tannins. In addition, metabolites, such as L-Homocysteine, L-Histidine, and L-Homomethionine, showed more than ten-fold difference in relative abundance from 30 to 100 days after SPD treatment, however, there were no significant changes after water treatment. The present study reveals novel metabolites involved in

mango FI in response to SPD, which would provide a theoretical basis for utilizeing SPD to induce mango flowering.

1 Widely targeted metabolite profiling of mango stem
2 apex during floral induction by compond of mepiquat
3 chloride, prohexadione-calcium and uniconazole

4 Fei Liang [1,2], Wentian Xu [1], Hongxia Wu [1], Bin Zheng [1], Qingzhi Liang [1], Yingzhi Li [2] and
5 Songbiao Wang [1]

6 [1] Key Laboratory of Tropical Fruit Biology of Ministry of Agriculture, South Subtropical Crops
7 Research Institute, Chinese Academy of Tropical Agricultural Sciences, Zhanjiang 524091,
8 China
9 [2] Binhai Agricultural College of Guangdong Ocean University, Zhanjiang 524088, China
10 Corresponding Author:
11 Yingzhi Li[2] and Songbiao Wang[1]

12 **Email address: liyz@gdou.edu.cn (Yingzhi Li); wsbcjy@163.com (Songbiao Wang)**

14 Abstract

15 **Background:** Insufficient low temperatures in winter and soil residues caused by paclobutrazol
16 (PBZ) application to induce flower pose a big challenge for mango production. Our previous
17 research discovered that SPD (compound of mepiquat chloride, prohexadione-calcium and
18 uniconazole), a gibberellin inhibitor, had a significant effect of improving the flowering and
19 yield of mango during two consecutive years of experiments (2020-2021). Researches have
20 indicated that flower induction (FI) is regulated at the metabolic level; However, little is known
21 about the metabolic changes during FI in response to SPD treatment.
22 **Methods:** Here, ultra-performance liquid chromatography-electrospray ionization-tandem mass
23 spectrometry (UPLC-ESI-MS/MS)-based widely targeted metabolomic analysis was carried out
24 to assess the metabolic differences in the mango stem apex during different stages of mango FI
25 by SPD or water treatment.
26 **Results:** A total of 582 compounds were annotated and 372 metabolites showed at least two-fold
27 differences in abundance (Variable Importance in Projection, VIP $\geqslant$ 1 and Fold change, FC$\geqslant$2
28 or$\leqslant$0.5) between buds at 30, 80, 100 days after SPD/water treatment or between buds under
29 different treatments. Lipids, phenolic acids, amino acids, carbohydrates and vitamins were
30 among the metabolites that showed significant differences over time after SPD treatment. 18 out
31 of 20 lipids, including lysophosphatidylethanolamine (12, LPE), lysophosphatidylcholine (7,
32 LPC), and free fatty acids (1, FA), were significantly up-regulated from 80 to 100 days after SPD
33 treatment compared to water treatment. Meanwhile, the release of dormancy in mango buds
34 observed at 80 to 100 days after SPD treatment was accompanied by the accumulation of proline,
35 ascorbic acid, carbohydrates and tannins. In addition, metabolites, such as L-Homocysteine, L-

36   Histidine, and L-Homomethionine, showed more than ten-fold difference in relative abundance
37   between 30 and 100 days after SPD treatment, however, there were no significant changes after
38   water treatment. The present study reveals novel metabolites involved in mango FI in response to
39   SPD, which would provide a theoretical basis for utilizing SPD to induce mango flowering.
40   **Keywords:** Mango; floral induction; metabolite; lipid; amino acid

Introduction

43   Mango (*Mangifera indica* L.) is one of the most important fruit crops in the tropical and
44   subtropical regions (He et al., 2021). China is the second largest mango production country (Li et
45   al., 2019). Floral induction (FI) is an essential development event in perennial woody fruit trees,
46   which determines the onset of fruit and plays a crucial role in fruit yield (Wilkie, Sedgley &
47   Olesen, 2008). Mango FI starts from dormant bud or growing bud and ends with the beginning of
48   flower bud morphological differentiation (commonly known as brush head in production).
49   Although the mechanisms that control flowering remain primarily unknown in mango, it can be
50   induced by low temperatures (Davenport, 2007). However, insufficient cold winter temperatures
51   due to global warming have affected mango FI and resulted in reduced fruit production in
52   commercial mango orchards in China, mainly in Hainan, Guangdong and Guangxi.
53   In recent decades, soil drenching of paclobutrazol (PBZ) has been used as a major practice
54   to induce mango flowering in many commercial mango orchards, including Guangdong,
55   Guangxi and Hainan in China. PBZ inhibits gibberellin biosynthesis and vegetative growth,
56   resulting in mango FI (Guevara, Jiménez & Bangerth, 2012). However, excessive doses of PBZ
57   over a long period can result in soil residues (Milfont et al., 2008; Silva et al., 2017), new bud
58   and panicle compaction, and increased disease occurrence (Singh & Bhattacherjee, 2005;
59   Coelho, 2014). Specifically, mango inflorescence malformation damages the mango industry and
60   threatens mango productivity(Freeman et al., 2014; Ansari et al., 2015). It also strongly affects
61   the normal growth of plants and human health (Jiang et al., 2019; Guo et al., 2020). In addition,
62   PBZ has a low mobility in the soil, so plants cannot fully absorb it, and therefore it will remain in
63   the soil for a long time. It will lead to pollution of surface water and groundwater resources
64   (Sharma & Awasthi, 2005; Silva et al., 2017). In addition to PBZ, there are several safer
65   gibberellin inhibitors such as uniconazole, prohexadione calcium and mepiquat chloride which
66   play roles in regulating plant growth. Uniconazole can inhibit the activity of ent-kaurene oxidase
67   (KO) in gibberellin biosynthesis and promote flowering of juvenile macadamia trees (Nagao,
68   Ho-a & Yoshimoto, 1999; Rademacher, 2000). Prohexadione calcium hinders gibberellin (GA)
69   biosynthesis to retard the runner formation of strawberry (Hytönen et al., 2009; Kim et al., 2019).
70   Mepiquat chloride promotes cotton lateral root formation by inhibiting GA biosynthesis and
71   signal transduction (Wu et al., 2019). More importantly, they have the characteristics of low
72   toxicity and low residue in soil (Basak & Rademacher, 2000; Bazzi et al., 2003; Li et al., 2012;
73   Dong, Zhu & Chen, 2021; Huang et al., 2021). The effect of uniconazole is 4-10 times higher
74   than that of paclobutrazol, but its residue in soil is only 1/10 of that of paclobutrazol (Gilbertz,

75 1992; Barrett & Nell, 1992; Sellmer et al., 1999). Prohexadione calcium can be rapidly degraded
76 into water and carbon dioxide by microorganisms in the soil, and has no residual toxicity to
77 rotation plants and no pollution to the environment (Evans et al., 1998; Ilias & Rajapakse, 2005).
78 Whereas, the effects of these agents on mango flowering regulation have not been evaluated.
79   Studies have revealed that specific metabolites are involved in FI in perennial fruit trees.
80 However, these studies mainly focused on the carbohydrates and endogenous hormones in leaves
81 and flower buds and their changes during FI (Upreti et al., 2013, 2014; Xing et al., 2015).
82 Research has also evaluated the effects of metabolites such as sucrose and fulvic acid with PBZ
83 on FI (Du et al., 2017; dos Santos Silva et al., 2021). Meanwhile, early reports in mango showed
84 that other metabolites, such as amino acids and phenols, were involved in mango FI (Tiwari,
85 Patel & Pandey, 2018). Osuna-Enciso et al. reported higher amino acids content in mango flower
86 buds than in leaf buds, indicating the increased need for amino acid during flowering (Colegio de
87 Postgraduados et al., 2001; Zhang et al., 2022). Meanwhile, in Arabidopsis, the increase in
88 phosphatidylcholine (PC) levels in the stem meristems accelerated flowering while the decrease
89 in PC levels in the stem meristems delayed flowering, indicating a correlation between PC levels
90 and the flowering time (Nakamura et al., 2014, 2019). However, the metabolic changes during
91 the different stages of mango FI, determined by a metabolomics approach, have not been
92 reported.
93   Metabolomics is an emerging 'omics' tool following genomics, transcriptomics, and
94 proteomics. Researchers have used widely targeted metabolite analysis based on tandem mass
95 spectrometry (MS/MS) data for large-scale metabolite profiling in various plant species (Wang et
96 al., 2018a, 2021; Zou et al., 2020; Yi et al., 2021; Xiao et al., 2021). Plant primary metabolites,
97 including sugars, amino acids, lipids, nucleotides, and other substances, act as essential
98 substances and energy sources for plant growth, development and reproduction. Based on the
99 ultra-performance liquid chromatography-tandem mass spectrometry (UPLC-MS/MS) detection
100 technology, a secondary spectral matching method was developed for the qualitative and
101 multiple reaction monitoring (MRM) of substance relative content, using an independently
102 constructed plant primary metabolite database. The metabolites were evaluated using both
103 univariate and multivariate statistical methods.
104   In this study, we evaluated the effects of SPD, a compound chemical composed of
105 uniconazole, prohexadione calcium and mepiquat chloride, on the flowering and yield of mango,
106 and we recorded the morphological characteristics of buds at different days (30, 60, 80, 100)
107 after SPD/water treatment. In addition, a UPLC-MS/MS analysis was performed to obtain a
108 comprehensive and dynamic metabolic profile, identify specific metabolites, and explore the
109 critical metabolic pathways in response to SPD treatment during mango FI. The findings will
110 provide a potential method for mango flowering management in subtropical regions and provide
111 a theoretical basis for applying SPD to regulate mango flowering.

112 **Materials & Methods**
113 **Plant material**

114   The experimental orchard is a commercial orchard, and the orchard adopts conventional
115   management measures. Except for a brief temperature drop in mid-December (below 15°C for
116   about one week), the average monthly temperature for the other months is higher than 15°C.
117   Before flowering, branches were not pruned and flies were bred in the orchard to pollinate. In
118   our pre-experiment, we sprayed about 12 L of water on the leaves of nine trees. Eighteen
119   randomly selected fifteen-year-old 'Tainong' mango trees (*Mangifera indica* L.) grown at the
120   commercial orchard at the South Subtropical Crops Research Institute of the Chinese Academy
121   of Tropical Agricultural Science in Zhanjiang, China (110° 16′ E, 21° 10′ N) were used in
122   this study from 2019 to 2021. In late September of years 2019 and 2020, when the leaves of the
123   second flush turned green, nine trees were selected and their leaves were sprayed with 12 L of
124   SPD (mepiquat chloride: 2 g. L-1, prohexadione-calcium: 100 mg. L-1, uniconazole: 300 mg.L-1
125   (researchers developed the formula for exogenous gibberellin inhibitors.) or 12L of water (as a
126   control) on the leaves of each tree, respectively. All other measures are routine management
127   measures. The experiments were conducted in a randomized block design with 3 repetitions per
128   treatment and 3 trees per repetition.
129   According to the classification of mango phenological growth stages described by Rajan
130   and Ramírez (Rajan et al., 2011; Ramírez et al., 2014), researchers still do not know the detail
131   information about the phonological changes from dormant bud to flower bud initiation stage.
132   Thus, morphological changes in the bud are regularly observed and photographed until the bud is
133   released. We also refer to Yang et al. for making paraffin sections and observing them (Oliveira
134   et al., 2020). Stage 1 is the dormant stage when the buds are dormant, about 30-60 days after
135   SPD/water treatment. Stage 2 is the green tip stage, about 60-80 days after SPD/water treatment.
136   During this stage, the swelling buds expose the inner leaf primordia under the SPD treatment but
137   still dormant buds under the water treatment. Stage 3 is bud initiation stage, about 80-100 days
138   after SPD/water treatment. At this stage, the apex of the mango stem is covered by elongated
139   bracts when treated with SPD, but the buds remain dormant until 100 days after water treatment.
140   After that, buds entered the stage of morphological differentiation according to Oliveira (2020)
141   under the SPD treatment but were still in dormancy under the control. Terminal buds were
142   collected at three different stages shown in Fig. 1 (30, 80 and 100 days after SPD/water
143   treatment) from October 2020 to January 2021. Experiments were carried out on three stages of
144   buds with three biological replicas. Each biological replica consists of a pool of 12 buds from
145   three trees. The bud samples collected were immediately placed in liquid nitrogen and stored in a
146   freezer at −80 °C.
147   We tagged a total of 20 branches evenly distributed on the east, west, north and south sides
148   of each tree, and we recorded the branches with flowers as flowering branches for each tree.
149   About 140 days after SPD/water treatment, the flower formation rate was evaluated using the
150   ratio of the number of flowering branches in the entire tree to the total number of branches in
151   each tree. When the fruit reached commercial harvest maturity, we calculated the mango yield
152   per tree. There are nine trees for SPD and water treatment respectively.
153 **Metabolite detection**

154   Metabolite extraction: Bud samples were pre-treated and extracted as previously described
155 (Wang et al., 2018b). Briefly, the frozen bud samples mentioned above were lyophilized and
156 smashed with zirconia beads in a mixer mill (MM 400, VERDER RETSCH, Shanghai, China)
157 for 1.5 min. Then, 0.1 g of sample powder was extracted in 1.2 mL 70% methanol solution
158 overnight at 4°C. The supernatant obtained after centrifugation at 12,000 rpm for 10 min was
159 passed through a CNWBOND Carbon-GCB SPE Cartridge (250 mg, 3 mL; ANPEL, Shanghai,
160 China) and filtered (0.22μm pore size; SCAA-104). L-2-chlorophenylalanine was used as the
161 standard solution in the study.

162   UPLC conditions: The bud extract was analyzed using an ultra-performance liquid
163 chromatography-electros pray ionization-tandem mass spectrometry (UPLC-ESI-MS/MS;
164 Shanghai, China) system (UPLC, SHIMADZU NexeraX2; MS, Applied Biosystems 4500 Q
165 TRAP). First, the aliquot (4 μL) was injected into the Agilent SB-C18 column (1.8 μm, 2.1
166 mm×100 mm) in an UPLC system. During sample analysis, the composition and the ratio of
167 mobile phases were changed slightly (Zou et al., 2020). The separation was achieved using the
168 mobile phases solvent A (pure water with 0.1% formic acid) and solvent B (acetonitrile with
169 0.1% formic acid) and a gradient program as follows: the starting conditions of 95% A, 5% B.
170 Within 9 min, a linear gradient to 5% A, 95% B was programmed, and a composition of 5% A,
171 95% B was kept for 1 min. Subsequently, a composition of 95% A, 5.0% B was adjusted within
172 1.10 min and kept for 2.9 min. The flow velocity was set at 0.35 ml per minute. The column
173 oven was set to 40 ℃.

174   ESI-Q TRAP-MS/MS: The effluent was alternatively connected to an AB4500 Q TRAP
175 UPLC/MS/MS system, equipped with an ESITurbo Ion-Spray interface, operating in both
176 positive and negative ionmodes and controlled by Analyst software (v1.6.3; AB Sciex). The
177 operating parameters were similar to those in the previous study (Zhang et al., 2020). An ion
178 source temperature of 550 °C and ion spray voltage (IS) of 5500 V (positive ion mode)/-4500 V
179 (negative ion mode) were used; ion source gas I (GSI), gas II(GSII), and curtain gas (CUR) were
180 set at 50, 60, and 25.0 psi, respectively. Finally, a specific set of MRM transitions were
181 monitored for each period according to the metabolites eluted within this period.

Qualitative and quantitative analyses of metabolites

183   Qualitative analysis: The MS data were analyzed based on the self-built database of purified
184 metabolite standards and the public metabolite database in collaboration with the MWDB
185 (MetWare Biotechnology Co., Ltd., Wuhan, China). The accurate precursor ion (Q1) and
186 production (Q3) values, retention times, and fragmentation patterns were compared with those of
187 the standards to analyze the primary and secondary MS information, followed by the removal of
188 few repeated signals (Zheng et al., 2021).

189   Quantitative analysis: The quantitative analysis was carried out using the MRM mode of the
190 triple quadrupole (QQQ) MS. The ions corresponding to other molecular weight substances were
191 initially excluded to avoid interference, and the parent ions of the target substances in the MRM
192 mode were searched, leading to higher precision and repeatability of results.

193 The peak area of all substance mass peaks was integrated after metabolite mass
194 spectrometry data from several samples were obtained, and the peaks of the same metabolite in
195 various samples were integrated and corrected. The relative content of metabolites is the integral
196 value of the peak area. Quality control samples (QC) samples are prepared by mixing extracts
197 from sample samples and are used to analyze sample repeatability within the same treatment
198 environment. A quality control sample is inserted into every ten test analysis samples during the
199 analysis to ensure that the process is repeatable.

200 **Statistical analysis**

201 The peak areas for each metabolite were normalized by unit variance (UV) scaling. The
202 normalized metabolite data of all samples were analyzed using principal component analysis
203 (PCA) by the statistics function of prcomp within R (v3.63) (www.r-project.org), hierarchical
204 cluster analysis (HCA) by the pheatmap in R package (v1.0.12). The relative abundance of all
205 differential metabolites was normalized by z-score, followed by K-Means clustering analysis by
206 R, and orthogonal projections to latent structures-discriminant analysis (OPLS-DA) by
207 MetaboAnalystR (v1.0.1) package in R (Thévenot et al., 2015) were used to evaluate the
208 metabolic differences between and within bud samples. The variable importance in the
209 projection (VIP) in the OPLS-DA model was used to identify the differential metabolites (VIP $\geq$
210 1 and absolute log2FC|fold change| $\geq$1). Annotated metabolites were mapped to the KEGG
211 database (http://www.kegg.jp/kegg/pathway.html) to determine the pathway associations.
212 Metabolite set KEGG enrichment analysis was performed on the pathways enriched with
213 significantly regulated metabolites; the pathways with Bonferroni corrected P-values $\leq$ 0.05 were
214 considered significantly enriched.

215

216 **Results**

217 **SPD treatment enhanced flowering rate and yield**

218 We investigated flowering rate and yield per tree of mango trees treated with SPD and water
219 for two consecutive years (2020-2021) (Fig. 2 and Supplemental Table S1). In 2020 and 2021,
220 the flowering rate and mango yield per tree of SPD treatment were significantly higher than
221 those of the control, and the flowering rate for two consecutive years exceeded 80%. In 2021, the
222 number and yield of mangos per tree treated by SPD decreased slightly compared with that in
223 2020, which may be due to some other factors, such as unfavourable temperature and rainfall.
224 The results confirmed the efficiency of SPD on mango flower induction.

225

226 **Morphological characteristics of buds in response to SPD treatment**

227 Both environmentally induced dormant bud and the growing bud can initiate floral bud in
228 mango (Batten & Mcconchie, 1995). Growing points of mango buds were covered by green or
229 brownish scales, which is different from the buds of some tropical evergreen perennials, such as
230 litchi, which are naked (Zhang et al., 2016). With the maturation of the second flush, the dormant
231 buds were thin and covered with green scales that tightly embraced each other, and the stem

232   apices were concealed during 30 and 60 days after treatment with SPD/water (Figs. 1 T-30/C-30,
233   T-60/C-60). Then, the buds started swelling and exposing the inner leaf primordia at 80 days
234   after SPD treatment, but no obvious changes were observed in buds treated with water (Figs. 1
235   T-80/C-80). Finally, the scales separated, and the base of mango bud is enlarged and the top is
236   pointed (a situation that indicates potential inflorescence formation) at 100 days after SPD
237   treatment, but scales of the bud only slightly loosened under the water control (Figs. 1 T-100/C-
238   100). After that, the first floral primordia were visible, and the panicles started to develop at 120
239   days after SPD treatment, whereas, scales of the bud treated with water were still mildly
240   separated (Figs. 1 T-120/C-120). In order to further confirm the flower bud differentiation stage
241   under SPD treatment, the terminal buds of 30 days, 60 days, 80 days, 100 days, and 120 days
242   after SPD treatment were analyzed by histological cytology. The stem apex meristem was dome-
243   shaped at 30-60 days after water/SPD treatment, then expanded laterally and lost its dome shape
244   at 80 days after water/SPD treatment. 100 days after SPD treatment, inflorescence primordia
245   appeared in the stem apex of the major axis and lateral axis, displaying a typical inflorescence
246   structure, a sign of flower bud morphological differentiation stage. The stem apex of water
247   treatment remained in the dormant stage.
248   During this morphogenic process, a targeted metabolomic analysis was conducted by
249   collecting mango buds at different stages of induction, eg. at 30 days after treatment with
250   SPD/water (TA/A), 80 days after treatment with SPD/water (TB/B), and 100 days after treatment
251   with SPD/water (TC/C), respectively, to investigate the metabolic dynamics during FI.
252

Metabolic characteristics of buds at different days in response to SPD treatment

255   In total, 582 metabolites were annotated from the mango buds at 30, 80, 100 days after
256   SPD/water treatment (Supplemental Table S2). A PCA was conducted on the 582 metabolites,
257   with PC1 and PC2 explaining 39.62% and 19.31% of the total variation, respectively. Lipids and
258   phenolic compounds are the main contributions to PC1, such as LysoPC 18:3, LysoPC 18:2,
259   LysoPC 16:2, Methyl gallate, Digallic acid, 1,3,6-Tri-O-galloyl-β-D-glucose, 4-O-Methylgallic
260   Acid and L-Malic acid-2-O-gallate. Phenolic compounds and organic acids are the main
261   contributions to PC2, such as 2-Hydroxycinnamic acid, 3-Hydroxycinnamic Acid, Trans-5-O-(p-
262   Coumaroyl)shikimate, Phenyl acetate, 2-Hydroxy-2-methyl-3-oxobutanoic acid, 2-
263   Methylsuccinic acid, 4-Hydroxy-2-Oxopentanoic Acid and Monomethyl succinate. The 18 bud
264   samples from 3 stages of two treatments distributed into distinct clusters, implying differences in
265   the metabolic characteristics among the bud at 30, 80, 100 days after SPD/water treatment. It is
266   consistent with the change of phenotypic characteristics (Fig. 3A). Besides, the r values
267   (correlation coefficient) of the biological repeats were greater than 0.97, while the correlation
268   between the different samples was low, indicating relatively good sample repeatability (Fig. 3B).
269   Further, a log10 transformation of peak area was applied to each metabolite to eliminate the
270   effects of quantity on pattern recognition, and an HCA analysis was performed. This analysis
271   revealed six distinct groups associated with TA, TB, TC, A, B and C, respectively. The content

272 of metabolites in groups 1 and 2 was the highest in samples of 100 days after water treatment;
273 that in groups 3 and 4 was the highest in samples of 30 or 80 days after water treatment; that in
274 groups 5 was the highest in samples of 80 and 100 days after SPD treatment; and that in groups 6
275 was the highest in samples of 100 days after SPD/water treatment (Fig. 3C). Thus, the PCA and
276 HCA analysis revealed differences in various metabolite spectrums among bud samples of
277 different stages and treatments with good reproducibility and stability.

278   Subsequently, the metabolites showing an FC ≥ 2 (up-regulated) or ≤ 0.5 (down-regulated)
279 between the A and B, the A and C, the B and C, the TA and TB, the TA and TC, the TB and TC,
280 the A and TA, the B and TB, and the C and TC were selected for further analysis to identify the
281 differential metabolites in the mango buds at different days after SPD/water treatment or in buds
282 under different treatments. The VIP value from the OPLS-DA model (VIP ≥ 1) was used to
283 screen these metabolites, and a total of 372 metabolites were identified from the nine
284 comparisons. Among these, 143 differential metabolites (36 up-regulated and 107 down-
285 regulated) were identified between A and B; 105 differential metabolites (23 up-regulated and 82
286 down-regulated) were identified between A and C; 20 differential metabolites (13 up-regulated
287 and 7 down-regulated) were identified between B and C; 131 differential metabolites (73 up-
288 regulated and 58 down-regulated) were identified between TA and TB; 151 (113 up-regulated
289 and 38 down-regulated) between TA and TC; and 224 (155 up-regulated and 69 down-regulated)
290 between TB and TC, 22 differential metabolites (7 up-regulated and 15 down-regulated) were
291 identified between A and TA, 101 differential metabolites (72 up-regulated and 29 down-
292 regulated) were identified between B and TB, 252 differential metabolites (179 up-regulated and
293 73 down-regulated) were identified between B and C (Fig. 4A). Furthermore, there were 14
294 differential metabolites constantly altered by water treatment, and 53 differential metabolites
295 continuously altered by SPD treatment. Compared with the control, 7 common metabolites were
296 found in buds at 30, 80 and 100 days after SPD/water treatment (Fig. 4B-D).

KEGG classification and enrichment analysis of differential
metabolites

299   Furthermore, the differential metabolites (between A and TA: 22, B and TB: 101 and C and
300 TC: 252) were mapped to the KEGG database. The results demonstrated that most of the
301 metabolites were related to the metabolism and biosynthesis of secondary metabolites. Few
302 metabolites were associated with the biosynthesis of amino acids. The remaining pathways
303 included ABC transporters, 2-oxocarboxylic acid metabolism, and aminoacyl-tRNA
304 biosynthesis, only the least proportion of metabolites were represented. Subsequently, KEGG
305 enrichment analysis of the differential metabolites was done to determine the differences in
306 metabolic pathways between the A and TA stages, the B and TB stages, the C and TC stages.
307 The enrichment analysis showed that the metabolites derived from glycine serine and threonine
308 metabolism, Cysteine and methionine metabolism, Zeatin biosynthesis, biosynthesis of amino
309 acids, Glycerolipid metabolism, Tryptophan metabolism, Phenylalanine tyrosine and tryptophan
310 biosynthesis, Carbon fixation in photosynthetic organisms and Arginine and proline metabolism

311 were significantly different between the B and TB stages, the C and TC stages ($p < 0.05$) (Fig. 5
312 and Supplemental Table S3).

313

K-means clustering analysis of differential metabolites

315 The average of three repeated relative abundances of all differential metabolites in each
316 sample was standardized by z-score and analyzed by K-means clustering to obtain the
317 accumulation pattern of the differential metabolites across the different stages of mango FI (Fig.
318 6 and Supplemental Table S4). The 372 differential metabolites (125 phenolic acids, 78 lipids,
319 52 amino acids and derivatives, 36 nucleotides and derivatives, 42 organic acids, and 39 others)
320 were divided into six clusters. Among them, the phenolic acids were classified into the cluster 2,
321 3, 4, 6 and 8 (12.8%, 12.8%, 12.8%, 12.8% and 19.2%), lipids were classified into the cluster 4
322 and 7 (26.9% and 33.3%), amino acids and derivatives were mainly classified into the cluster 4
323 and 6 (32.6% and 26.9%), nucleotides and derivatives were classified into the cluster 4 (30.5%),
324 organic acids were classified into the cluster 1 and 3 (16.7% and 19%), and others were
325 classified into the cluster 3 and 6 (33.3% and 25.6%).

Identification of lipids, phenolic acids, and amino acids during FI after SPD treatment

328 To select metabolites that might be related to FI instead of SPD treatment, we focused on
329 metabolites with significant differences during FI in response to SPD treatment, comparing their
330 accumulation patterns after different days both by SPD and water treatment. The present study
331 identified 53 metabolites (Supplemental Table S5) during FI that showed significant changes
332 from TA to TB and TB to TC after SPD treatment, including 20 lipids, 18 phenolic acids, 7
333 amino acids and their derivatives, 5 nucleotides and their derivatives, 2 organic acids, and 1 other
334 (Fig. 7A). The results suggested that these metabolites, especially lipids, phenolic acids, and
335 amino acids, might play a key role in FI in respond to SPD treatment in mango. 20 differently
336 changed lipids included 12 lysophosphatidylethanolamine, 7 lysophosphatidylcholine, and 1 free
337 fatty acid. 18 out of the 20 lipids showed a significant decrease towards TB and a substantial
338 increase towards TC following SPD treatment, but a significant decrease towards B and no
339 alterations towards C after water treatment. The result indicated the significance of lipids
340 decomposition and synthesis during mango FI by SPD treatment. Meanwhile, 12 out of 18
341 phenolic acids significantly increased from TA to TB and then to TC under SPD treatment, but
342 had no significant changes from A to B then to C with water treatment. Among them, four tannin
343 compounds (1,4,6-tri-O-galloyl-β-D-glucose, 1,3,6-tri-O-galloyl-β-D-glucose, 2,4,6-tri-O-
344 galloyl-D-glucose, and 1,2,3,6-tetra-O-galloyl-β-D-glucose) were continuously increased from
345 TA to TB and then to TC, and their relative abundances were higher than other phenolic acids at
346 all stages after SPD treatment. Besides, the seven amino acids significantly increased with FI
347 following SPD treatment and had no significant changes at all stages with water treatment); L-
348 homoserine (the precursor of ethylene), L-serine, and L-threonine were the most abundant under

349   the SPD treatment. In addition, the proline and its premise substances involved in the
350   biosynthesis of amino acids presented a continuous increase (TA to TB to TC) following SPD
351   treatment, however, showed no significant changes (A to B to C) after water treatment (Fig. 7B).

352

Identification of carbohydrates and vitamins during FI after SPD treatment

355   Additionally, 7 vitamins and 11 saccharides and alcohols showing significant changes
356   between the TA and TC stages by SPD treatment were identified, and they showed different
357   accumulation patterns in samples of different days after SPD and water treatment (Fig. 7C and
358   Supplemental Table S6). Among the 11 saccharides and alcohols, 10 carbohydrates, including D-
359   fructose6-phosphate, D-fructose-1,6-biphosphate, glucose-1-phosphate, sorbitol-6-phosphate,
360   and D-glucose 6-phosphate, showed a sharp increase from TA to TC by SPD treatment but no
361   significant changes from A to C after water treatment. Among the 7 vitamins, erythorbic acid
362   and L-ascorbic acid, with the highest relative abundance, showed a substantial increase from TA
363   to TC following SPD treatment, while no significant changes from A to C by water treatment. In
364   addition, 14 out of 372 differential metabolites changed more than ten times at the different
365   stages of FI treated with SPD, but had no significant changes treated with water (Fig. 8 and
366   Supplemental Table S7); this group included L-Homocysteine (TA vs TB, TA vs TC), L-
367   Histidine (TA vs TC), and L-Homomethionine (TA vs TC, TB vs TC).

368

Discussion

370   Recently, the metabolic regulation of flower bud dormancy in temperate fruits has attracted
371   the attention of numerous researchers (Zhuang et al., 2015; Gabay et al., 2019; Yang et al.,
372   2021). The FI in mango, which is accompanied by the release of a dormant bud and regulated by
373   low temperatures (Núñez-Elisea & Davenport, 1995; Wilkie, Sedgley & Olesen, 2008; Ramírez
374   & Davenport, 2010), seems to be similar to the regulation of flower bud dormancy in temperate
375   fruit trees. However, knowledge of the changes in metabolites in mango buds from dormancy to
376   flower initiation is limited. The present study used UPLC-MS/MS-based widely targeted
377   metabolomics to reveal the overall dynamics of the primary metabolites in mango bud at three
378   representative stages of FI. A total of 582 metabolites were identified, of which 372 were
379   differentially accumulated during the three FI stages. Metabolites including lipids, phenolic
380   acids, amino acids, carbohydrates, and vitamins were further characterized. Notably, the analysis
381   revealed that metabolites such as proline changed significantly during FI in response to SPD
382   treatment. Thus, this study provides evidence for novel mechanisms underlying FI in mango.
383   In Zhanjiang, China, it is normal for some mango varieties to not blossom without any
384   treatment, such as Tainong-1 and Renong-1. Based on our results on fruit yield, we found that
385   the mango yield in 2021 was slightly lower than that in 2020. It may be caused by damage of
386   insect pests, plant pathogens, soil and water pollution, poor pollination, stresses of water and
387   temperature. Approximately 5–80% of mango yield losses in India are directly or indirectly

388 caused by fruit flies (Stonehouse, 2001). In recent years, mango leaf, branch, and fruit infections
389 by bacterial black spot have become increasingly serious in the mango-producing areas, resulting
390 in lower yields and product quality (Zhou et al., 2019). There is global evidence that salinity
391 pollution of soil and water reduces crop production (Haque, 2006). Pollination is vital for most
392 fruit trees, and poor pollination leads to poor fruit quality and low yield (Kleiman, Koptur &
393 Jayachandran, 2021). When crops are under-irrigated, they risk water stress, which can lead to a
394 reduction in yield or quality (Jabro et al., 2020). Temperature is essential in inducing flowering
395 in mango trees because bud growth occurs at temperatures of around 10 °C at night and 20 °C
396 during the day, resulting in flower buds(de los Santos-Villalobos et al., 2013).
397   The analysis of differential metabolites between different samples showed that the number
398 of differential metabolites in buds gradually increased with time after SPD treatment, while the
399 number in control buds gradually decreased. These results indicated that SPD treatment had an
400 important effect on metabolites in mango buds, and the effect was most significant at 80 and 100
401 days after the treatment. The metabolism changes were consistent with the morphological
402 development.
403   KEGG enrichment analysis revealed that floral induction of mango involved multiple
404 metabolic pathways. Zhang et al. discovered that a higher amino acid content was beneficial to
405 walnut flower induction (Zhang et al., 2022). Rachapudi et al. discovered that biosynthesis of
406 amino acids and 2-oxocarboxylic acid metabolism, carbon metabolism and fatty acid metabolism
407 were also involved in floral induction of *Pongamia pinnata* (Sreeharsha et al., 2016). Yan et al.
408 discovered that aminoacyl-tRNA biosynthesis was involved in floral induction of early-spring
409 plants (Yan et al., 2022). This study indicated that multiple metabolic pathways may jointly
410 regulate flowering induction in mango. Amino acid and lipids may play an important role. K-
411 means clustering analysis of differential metabolites revealed that levels of phenolic compounds
412 changed significantly during the 80-100 days following SPD treatment, but not in the 80-100
413 days following water treatment. It was demonstrated that phenolic acids promoted mango
414 blossoming (Srilatha & Reddy, 2015; Srilatha et al., 2016). In this study, lipids levels increased
415 significantly in the 80-100 days following SPD treatment, but not in the 80-100 days following
416 water treatment. Research has proposed that endogenous lipids of mango shoots have hormonal
417 activity and play an important role in mango flowering(Kumar, Ram & Pant, 1989). In this study,
418 amino acids levels increased significantly in the 30-100 days following SPD treatment, but not in
419 the 80-100 days following water treatment (Shivashankara, Geetha & Roy, 2019; Nj et al.). The
420 results showed these pathways respond to floral induction of mango (Prates et al., 2021).
421   Lipids are components of the cell membrane and play essential roles in regulating different
422 biological pathways (Quartacci et al., 1995; Hamrouni, Salah & Marzouk, 2001). Lipids in plants
423 can be divided into several categories, including glycerophospholipid (GP), glycerolipid (GL),
424 and fatty acyl (FA). GPs are further divided based on the head group structures into the
425 following classes: phosphatidylcholine (PC), phosphatidylethanolamine (PE), phosphatidylserine
426 (PS), phosphatidic acid (PA), phosphatidylinositol (PI), phosphatidylglycerol (PG), and
427 cardiolipin (CL). During bud dormancy in European pears, phospholipids significantly increased

428   with chilling accumulation (Gabay et al., 2019). Significant escalations in the LPC and LPE
429   content in the Arabidopsis leaves were observed in response to bacterial infection and low
430   temperatures. Meanwhile, an increase in phosphocholine, the precursor for the biosynthesis of
431   PC, was detected during flower bud dormancy release in black currant (Jung et al., 2017). In this
432   study, 18 lipids changed significantly following SPD treatment, and LPE 17:1 and LPE 15:1
433   showed more than ten-fold change from 80 to 100 days after SPD treatment, highlighting their
434   role in mango FI in response to SPD treatment. Interestingly, biochemical analysis in
435   Arabidopsis showed that FLOWERING LOCUS T protein (FT) binds to diurnally changing
436   molecular species of PC to promote flowering, indicating a role of PC in the timing of flowering
437   (Nakamura et al., 2014, 2019). However, the importance of lipid metabolism during FI treated
438   with SPD treatment of mango needs to be further studied by integrating relative gene
439   transcription analysis.

440   Phenolic compounds are another set of metabolites that play essential roles in regulating the
441   growth and development of plants (Halbwirth et al., 2006; Edwards et al., 2008). Phenolic acids
442   are organic acids with phenolic groups. The phenolic hydroxyl groups form stable phenoxy
443   radicals with free radicals and eliminate free radicals in vivo. Wild chokeberries and cultivar
444   "Viking" with higher phenolic acid content have intense anti-radical activity (Jakobek et al.,
445   2012). Oliveira et al. proved the apparent accumulation of phenolic compounds in mango stem
446   apex before flower bud initiation from the cytological point of view (Oliveira et al., 2020). In the
447   present study, phenolic acids accounted for a high proportion of the metabolites that showed
448   significant changes from 30 to 80 then to 100 days by SPD treatment. Most of them were
449   continuously increased, which may be involved in free radical scavenging. Meanwhile, studies
450   have proven that tannins and related compounds, including coumarin, trans-cinnamic acid, and
451   many phenolic compounds, are gibberellin antagonists (Corcoran, Geissman & Phinney, 1972).
452   Therefore, the up-regulated tannin compounds also probably antagonize gibberellin during
453   flower bud differentiation to promote flowering.

454   The release of bud dormancy is accompanied by proline accumulation (Seif El-Yazal, Seif
455   El-Yazal & Rady, 2014). Besides, free proline accumulation is a typical response of plants to
456   various stresses, maintaining the osmotic balance between cytoplasm and vacuole. Proline can
457   remove reactive oxygen species produced under stress and be used as an osmotic agent to protect
458   the subcellular structure (Zhuang et al., 2015). Studies have shown that the low levels of proline
459   in switchgrass delay flowering. In addition, proline is involved in flowering signals (Schwacke et
460   al., 1999; Mattioli et al., 2009; Kavi Kishor & Sreenivasulu, 2014; Kim et al., 2021). Transgenic
461   arabidopsis overexpressing Δ1-Pyrroline-5-carboxylate synthetase (AtP5CS1) bloomed early and
462   accumulated a large amount of proline under long-day and short-day conditions (Mattioli et al.,
463   2012). AtP5CS2 is a multi-allelic AtP5CS gene, an early target of CONSTANS (CO), and
464   participates in flower formation (Samach et al., 2000). Many differential metabolites were
465   related to amino acid biosynthesis in this study, and L-proline and its precursors increased
466   continuously during FI in response to SPD treatment (Fig. 7B), with high relative abundance per

467 stage. These observations indicated that the dormancy release of mango buds followed proline
468 accumulation.
469   Plants require carbohydrates for growth and development; they provide energy to maintain
470 the growth of buds after dormancy and link sugar signals with flowering-related pathways
471 (Zhuang et al., 2013; Chen et al., 2018). Jesús GuillamónGuillamón found that D-fructose-2-
472 phosphate and D-fructose-2,6-biphosphate in almond flower buds increased at the stages close to
473 endodormancy release (Guillamón et al., 2020). In this study, saccharides accumulated from 30
474 to 100 days of SPD treatment were mainly those substances related to starch and sucrose
475 metabolism. These findings indicate that the accumulation of saccharides (D-fructose 6-
476 phosphate,D-fructose-1,6-biphosphate, glucose-1-phosphate, and D-glucose 6-phosphate) may
477 be important in mango flower bud development after SPD treatment (Upreti et al., 2014).
478 Meanwhile, D-glucosamine 1-phosphate alone was decreased. Previous studies have shown that
479 glucosamine 6-phosphate may be metabolized to fructose 6-phosphate, increasing glycolysis flux
480 (Xing et al., 2008). In red-rice seeds, endodormancy release was associated with increased
481 glycolysis and energy obtained (Gianinetti et al., 2018). These findings are consistent with our
482 results in mango stem apex, indicating the role of the carbohydrate in FI.
483   Furthermore, erythorbic acid and L-ascorbic acid were abundant and continuously
484 accumulated vitamins from 30 to 100 days following SPD treatment, but no significant changes
485 were observed in the water treatment. Ascorbic acid is an important antioxidant and an auxiliary
486 factor for synthesizing few hormones (Barth, 2006; Bilska et al., 2019). It also links flowering
487 time with response to pathogens through a complex signal transduction network (Du et al.,
488 2016). In Japanese pear and sweet cherry, reactive oxygen species increased during
489 endodormancy and decreased after endodormancy release (Gianinetti et al., 2018; Baldermann et
490 al., 2018). Additionally, research has demonstrated that a rise in ascorbic acid levels with an
491 increase in flavonols is implicated in the degradation of hydrogen peroxide (H2O2) in grapevine
492 leaves (*Vitis vinifera* L.) (Pérez, 2002). Therefore, we speculate that ascorbic acid as an
493 antioxidant can scavenge free radicals, and its accumulation promotes mango flower bud
494 differentiation.
495   In addition to the substances mentioned above, a few other metabolites (Fig. 8), including L-
496 Homocysteine, L-Histidine, and L-Homomethionine et al., may also play important roles in some
497 specific stages. The relative abundance of these metabolites changed more than ten folds at a
498 particular stage after SPD treatment. The significant changes in the relative abundance of these
499 metabolites during FI in response to SPD treatment indicate their role in mango FI. Further
500 analysis of the role of these metabolites may clarify the molecular mechanism of mango FI by
501 SPD treatment.
502

Conclusions

504   In this study, we confirm the positive role of SPD in promoting mango flowering.
505 Significant changes in the abundances of metabolites such as lipids, tannins, proline, ascorbic
506 acid, and saccharides were detected in the buds from 30 to 80 and then to 100 days after SPD

507 treatment, indicating their crucial role during mango FI in response to SPD treatment. The results
508 will provide a novel approach to mango flowering management in subtropical regions and
509 provide a theoretical basis for applying SPD to regulate mango flowering.
510

Acknowledgements

Author Contributions: Fei Liang and Wentian Xu contributed equally to this work. Songbiao
Wang and Yingzhi Li are corresponding authors. Songbiao Wang, Yingzhi Li, Wentian Xu and
Fei Liang conceived and designed the study. Fei Liang, Hongxia Wu and Qingzhi Liang
performed the experiments and field evaluations, Fei Liang, Wentian Xu and Bin Zheng
analyzed the data. Fei Liang drafted the initial text with contributions from the other authors;
Songbiao Wang, Wentian Xu and Yingzhi Li revised the manuscript. All authors have read and
approved the final manuscript.

Funding: This research was funded by the National Key R & D Program of China (No.
2020YFD1000604, 2019YFD1000500), Hainan Province Natural Science Foundation of China
(320QN323), Guangdong Provincial Special Fund for Modern Agriculture Industry Technology
Innovation Teams (2019KJ108), and the Project of Enhancing School With Innovation of
Guangdong Ocean University (GDOU2013050217, GDOU2016050256).

Acknowledgments: The authors thank Wuhan Metware Biotechnology Co., Ltd., for widely
targeted metabolomics analysis. We acknowledge TopEdit LLC for the linguistic editing and
proofreading during the preparation of this manuscript.

527 **Conflicts of Interest:** The authors declare that they have no conflicts of interest.
528

References

530 Ansari MW, Rani V, Shukla A, Bains G, Pant RC, Tuteja N. 2015. Mango (*Mangifera indica L.*)

531   malformation: a malady of stress ethylene origin. Physiology and Molecular Biology of

532   Plants 21:1–8. DOI: 10.1007/s12298-014-0258-y.

533 Baldermann S, Homann T, Neugart S, Chmielewski F-M, Götz K-P, Gödeke K, Huschek G,

534   Morlock G, Rawel H. 2018. Selected Plant Metabolites Involved in Oxidation-Reduction

535   Processes during Bud Dormancy and Ontogenetic Development in Sweet Cherry Buds

536   (*Prunus avium L.*). Molecules 23:1197. DOI: 10.3390/molecules23051197.

537 Barrett JE, Nell TA. 1992. Efficacy of Paclobutrazol and Uniconazole on Four Bedding Plant

538   Species. HortScience 27:896–897. DOI: 10.21273/HORTSCI.27.8.896.

539   Barth C. 2006. The role of ascorbic acid in the control of flowering time and the onset of

540   senescence. Journal of Experimental Botany 57:1657–1665. DOI: 10.1093/jxb/erj198.

541   Basak A, Rademacher W. 2000. GROWTH REGULATION OF POME AND STONE FRUIT

542   TREES BY USE OF PROHEXANEDIONE-CA. Acta Horticulturae:41–50. DOI:

543   10.17660/ActaHortic.2000.514.4.

544   Batten D, Mcconchie C. 1995. Floral Induction in Growing Buds of Lychee (*Litchi chinensis*)

545   and Mango (Mangifera indica). Functional Plant Biology 22:783. DOI:

546   10.1071/PP9950783.

547   Bazzi C, Messina C, Tortoreto L, Stefani E, Bini F, Brunelli A, Andreotti C, Spinelli F, Costa G,

548   Hauptmann S, Stammler G, Doerr S, Marr J, Rademacher W. 2003. Control of Pathogen

549   Incidence in Pome Fruits and Other Horticul- tural Crop Plants with Prohexadione-Ca. :7.

550   Bilska K, Wojciechowska N, Alipour S, Kalemba EM. 2019. Ascorbic Acid—The Little-Known

551   Antioxidant in Woody Plants. Antioxidants 8:645. DOI: 10.3390/antiox8120645.

552   Chen X, Qi S, Zhang D, Li Y, An N, Zhao C, Zhao J, Shah K, Han M, Xing L. 2018.

553   Comparative RNA-sequencing-based transcriptome profiling of buds from profusely

554   flowering 'Qinguan' and weakly flowering 'Nagafu no. 2' apple varieties reveals novel

555   insights into the regulatory mechanisms underlying floral induction. BMC Plant Biology

556   18:1–21. DOI: 10.1186/s12870-018-1555-3.

557   Coelho EF. 2014. Flowering and fruit set of mango in different doses of paclobutrazol (PBZ).

558   Enciclopédia Biosfera 10:7.

559   Colegio de Postgraduados, Osuna-Enciso T, Becerril-Román AE, Mosqueda-Vázquez R,

560   Villarreal-Romero M, Castillo-Morales A. 2001. PROMOTORES DE FLORACIÓN Y

561   CONCENTRACIÓN DE ALMIDÓN Y AMINOÁCIDOS EN YEMAS DE MANGO.

562   Revista Chapingo Serie Horticultura VII:209–215. DOI: 10.5154/r.rchsh.2000.08.059.

563   Corcoran MR, Geissman TA, Phinney BO. 1972. Tannins as Gibberellin Antagonists. Plant

564   Physiology 49:323–330. DOI: 10.1104/pp.49.3.323.

565   Davenport TL. 2007. Reproductive physiology of mango. Brazilian Journal of Plant Physiology

566   19:363–376. DOI: 10.1590/S1677-04202007000400007.

567   Dong Z, Zhu W, Chen L. 2021. Effects of uniconazole on stress resistance indices, metabolite

568   content and endogenous hormones of potted Paeonia lactiflora 'Dafugui.' Maejo Int. J.

569   Sci. Technol.:11.

570   Du D, Gao X, Geng J, Li Q, Li L, Lv Q, Li X. 2016. Identification of Key Proteins and Networks

571   Related to Grain Development in Wheat (*Triticum aestivum* L.) by Comparative

572   Transcription and Proteomic Analysis of Allelic Variants in TaGW2-6A. Frontiers in

573   Plant Science 7. DOI: 10.3389/fpls.2016.00922.

574   Du L, Qi S, Ma J, Xing L, Fan S, Zhang S, Li Y, Shen Y, Zhang D, Han M. 2017. Identification

575   of TPS family members in apple (*Malus x domestica Borkh*.) and the effect of sucrose

576   sprays on TPS expression and floral induction. Plant Physiology and Biochemistry

577   120:10–23. DOI: 10.1016/j.plaphy.2017.09.015.

578   Edwards WR, Hall JA, Rowlan AR, Schneider-Barfield T, Sun TJ, Patil MA, Pierce ML, Fulcher

579   RG, Bell AA, Essenberg M. 2008. Light filtering by epidermal flavonoids during the

580   resistant response of cotton to Xanthomonas protects leaf tissue from light-dependent

581   phytoalexin toxicity. Phytochemistry 69:2320–2328. DOI:

582   10.1016/j.phytochem.2008.05.021.

583 Evans JR, Evans RR, Regusci CL, Rademacher W. 1998. Mode of Action, Metabolism, and

584 Uptake of BAS 125W, Prohexadione-calcium. :2.

585 Freeman S, Shtienberg D, Maymon M, Levin AG, Ploetz RC. 2014. New Insights into Mango

586 Malformation Disease Epidemiology Lead to a New Integrated Management Strategy for

587 Subtropical Environments. Plant Disease 98:1456–1466. DOI: 10/gpj3hq.

588 Gabay G, Faigenboim A, Dahan Y, Izhaki Y, Itkin M, Malitsky S, Elkind Y, Flaishman MA.

589 2019. Transcriptome analysis and metabolic profiling reveal the key role of α-linolenic

590 acid in dormancy regulation of European pear. Journal of Experimental Botany 70:1017–

591 1031. DOI: 10.1093/jxb/ery405.

592 Gianinetti A, Finocchiaro F, Bagnaresi P, Zechini A, Faccioli P, Cattivelli L, Valè G, Biselli C.

593 2018. Seed Dormancy Involves a Transcriptional Program That Supports Early Plastid

594 Functionality during Imbibition. Plants 7:35. DOI: 10.3390/plants7020035.

595 Gilbertz DA. 1992. Chrysanthemum Response to Timing of Paclobutrazol and Uniconazole

596 Sprays. HortScience 27:322–323. DOI: 10.21273/HORTSCI.27.4.322.

597 Guevara E, Jiménez VM, Bangerth FK. 2012. Response of Endogenous Hormone

598 Concentrations to Two Floral Inductive Treatments, viz. KNO3 and PBZ, in Mango cv.

599 'Tommy Atkins' Growing Under Tropical Conditions. Tropical Plant Biology 5:253–

600 260. DOI: 10.1007/s12042-012-9107-8.

601 Guillamón JG, Prudencio ÁS, Yuste JE, Dicenta F, Sánchez-Pérez R. 2020. Ascorbic acid and

602 prunasin, two candidate biomarkers for endodormancy release in almond flower buds

603 identified by a nontargeted metabolomic study. Horticulture Research 7:203. DOI:

604 10.1038/s41438-020-00427-5.

605   Guo H-M, Zhao Y, Yang M-NO, Yang Z-H, Li J-H. 2020. The enantioselective effects and

606   potential risks of paclobutrazol residue during cucumber pickling process. Journal of

607   Hazardous Materials 386:121882. DOI: 10.1016/j.jhazmat.2019.121882.

608   Halbwirth H, Puhl I, Haas U, Jezik K, Treutter D, Stich K. 2006. Two-Phase Flavonoid

609   Formation in Developing Strawberry (*Fragaria × ananassa*) Fruit. Journal of

610   Agricultural and Food Chemistry 54:1479–1485. DOI: 10.1021/jf0524170.

611   Hamrouni I, Salah HB, Marzouk B. 2001. Effects of water-deficit on lipids of safflower aerial

612   parts. Phytochemistry 58:277–280. DOI: 10.1016/S0031-9422(01)00210-2.

613   Haque SAnwarul. 2006. Salinity problems and crop production in coastal regions of Bangladesh.

614   Pakistan Journal of Botany 38:1359–1365.

615   He R, Yang Y, Hu Z, Xue R, Hu Y. 2021. Resistance mechanisms and fitness of pyraclostrobin-

616   resistant isolates of Lasiodiplodia theobromae from mango orchards. PloS One

617   16:e0253659. DOI: 10/gpj5mc.

618   Huang K, Xiao Y, Dong Y, Xu X, Zhang R, Lin L, Liao M. 2021. Effects of uniconazole on the

619   physiological characteristics and cadmium accumulation of Cyphomandra betacea

620   seedlings. Environmental Progress & Sustainable Energy 40. DOI: 10.1002/ep.13614.

621   Hytönen T, Elomaa P, Moritz T, Junttila O. 2009. Gibberellin mediates daylength-controlled

622   differentiation of vegetative meristems in strawberry *(Fragaria × ananassa* Duch). BMC

623   Plant Biology 9:1–12. DOI: 10.1186/1471-2229-9-18.

624   Ilias IF, Rajapakse N. 2005. Prohexadione-calcium affects growth and flowering of petunia and

625   impatiens grown under photoselective films. Scientia Horticulturae 106:190–202. DOI:

626   10.1016/j.scienta.2005.02.023.

627   Jabro JD, Stevens WB, Iversen WM, Allen BL, Sainju UM. 2020. Irrigation Scheduling Based

628   on Wireless Sensors Output and Soil-Water Characteristic Curve in Two Soils. Sensors

629   (Basel, Switzerland) 20:1336. DOI: 10.3390/s20051336.

630   Jakobek L, Drenjančević M, Jukić V, Šeruga M. 2012. Phenolic acids, flavonols, anthocyanins

631   and antiradical activity of "Nero", "Viking", "Galicianka" and wild chokeberries.

632   Scientia Horticulturae 147:56–63. DOI: 10.1016/j.scienta.2012.09.006.

633   Jiang X, Wang Y, Xie H, Li R, Wei J, Liu Y. 2019. Environmental behavior of paclobutrazol in

634   soil and its toxicity on potato and taro plants. Environmental Science and Pollution

635   Research 26:27385–27395. DOI: 10.1007/s11356-019-05947-9.

636   Jung K, Fastowski O, Poplacean I, Engel K-H. 2017. Analysis and Sensory Evaluation of

637   Volatile Constituents of Fresh Blackcurrant (*Ribes nigrum* L.) Fruits. Journal of

638   Agricultural and Food Chemistry 65:9475–9487. DOI: 10.1021/acs.jafc.7b03778.

639   Kavi Kishor PB, Sreenivasulu N. 2014. Is proline accumulation per se correlated with stress

640   tolerance or is proline homeostasis a more critical issue?: Proline homeostasis. Plant, Cell

641   & Environment 37:300–311. DOI: 10.1111/pce.12157.

642   Kim JH, Kim MS, Prasad D, Jung WJ, Seo YW. 2021. Molecular characterization of the wheat

643   putative proline-rich protein TaELF7 and its involvement in the negative regulation of

644   Arabidopsis flowering. Journal of Plant Physiology 262:153439. DOI:

645   10.1016/j.jplph.2021.153439.

646   Kim H, Lee H, Kang J, Hwang S. 2019. Prohexadione-Calcium Application during Vegetative

647   Growth Affects Growth of Mother Plants, Runners, and Runner Plants of Maehyang

648   Strawberry. Agronomy 9:155. DOI: 10.3390/agronomy9030155.

649 Kleiman BM, Koptur S, Jayachandran K. 2021. Weeds Enhance Pollinator Diversity and Fruit
650   Yield in Mango. Insects 12:1114. DOI: 10.3390/insects12121114.

651 Kumar A, Ram S, Pant RC. 1989. Endogenous lipid of mango shoot and their significance in
652   flowering. Acta horticulturae.

653 Li Q, Bu J, Shu J, Yu Z, Tang L, Huang S, Guo T, Mo J, Luo S, Solangi GS, Hsiang T. 2019.
654   Colletotrichum species associated with mango in southern China. Scientific Reports
655   9:18891. DOI: 10.1038/s41598-019-54809-4.

656 Li W, Chen M, Chen W, Qiao C, Li M, Han L. 2012. Determination of mepiquat chloride in
657   cotton crops and soil and its dissipation rates. Ecotoxicology and Environmental Safety
658   85:137–143. DOI: 10.1016/j.ecoenv.2012.08.015.

659 Mattioli R, Biancucci M, Lonoce C, Costantino P, Trovato M. 2012. Proline is required for male
660   gametophyte development in Arabidopsis. BMC Plant Biology 12:236. DOI:
661   10.1186/1471-2229-12-236.

662 Mattioli R, Falasca G, Sabatini S, Altamura MM, Costantino P, Trovato M. 2009. The proline
663   biosynthetic genes *P5CS1* and *P5CS2* play overlapping roles in Arabidopsis flower
664   transition but not in embryo development. Physiologia Plantarum 137:72–85. DOI:
665   10.1111/j.1399-3054.2009.01261.x.

666 Milfont ML, Antonino ACD, Martins JMF, Netto AM, Gouveia ER, Correa MM. 2008.
667   Transporte do paclobutrazol em colunas de solos. Revista Brasileira de Ciência do Solo
668   32:2165–2175. DOI: 10.1590/S0100-06832008000500037.

669 Nagao MA, Ho-a EB, Yoshimoto JM. 1999. Uniconazole Retards Growth and Increases
670   Flowering of Young Macadamia Trees. HortScience 34:104–105. DOI:
671   10.21273/HORTSCI.34.1.104.

672 Nakamura Y, Andrés F, Kanehara K, Liu Y, Dörmann P, Coupland G. 2014. Arabidopsis
673   florigen FT binds to diurnally oscillating phospholipids that accelerate flowering. Nature
674   Communications 5:3553. DOI: 10.1038/ncomms4553.

675 Nakamura Y, Lin Y-C, Watanabe S, Liu Y, Katsuyama K, Kanehara K, Inaba K. 2019. High-
676   Resolution Crystal Structure of Arabidopsis *FLOWERING LOCUS T* Illuminates Its
677   Phospholipid-Binding Site in Flowering. iScience 21:577–586. DOI:
678   10.1016/j.isci.2019.10.045.

679 Nj G, Sj P, Ry K, Ni S, Sa H. Effect of time and width of girdling on flowering and yield of
680   mango (*Mangifera indica* L.) cv. Alphonso. International Journal of Chemical Studies:5.

681 Núñez-Elisea R, Davenport TL. 1995. Effect of leaf age, duration of cool temperature treatment,
682   and photoperiod on bud dormancy release and floral initiation in mango. Scientia
683   Horticulturae 62:63–73. DOI: 10.1016/0304-4238(94)00749-6.

684 Oliveira MB, Figueiredo MGF, Pereira MCT, Mouco MA do C, Ribeiro LM, Mercadante-
685   Simões MO. 2020. Structural and cytological aspects of mango floral induction using
686   paclobutrazol. Scientia Horticulturae 262:109057. DOI: 10.1016/j.scienta.2019.109057.

687 Pérez F. 2002. Ascorbic acid and flavonoid-peroxidase reaction as a detoxifying system of H2O2
688   in grapevine leaves. Phytochemistry 60:573–580. DOI: 10.1016/S0031-9422(02)00146-2.

689 Prates AR, Züge PGU, Leonel S, Souza JMA, Ávila J de. 2021. Flowering induction in mango
690   tree: updates, perspectives and options for organic agriculture. Pesquisa Agropecuária
691   Tropical 51:e68175. DOI: 10.1590/1983-40632021v5168175.

692 Quartacci MF, Pinzino C, Sgherri Clm, Navari-Izzo F. 1995. Lipid Composition and Protein
693   Dynamics in Thylakoids of Two Wheat Cultivars Differently Sensitive to Drought. Plant
694   Physiology 108:191–197. DOI: 10.1104/pp.108.1.191.

695   Rademacher W. 2000. G ROWTH R ETARDANTS : Effects on Gibberellin Biosynthesis and

696   Other Metabolic Pathways. Annual Review of Plant Physiology and Plant Molecular

697   Biology 51:501–531. DOI: 10.1146/annurev.arplant.51.1.501.

698   Rajan S, Tiwari D, Singh VK, Saxena P, Y.T.N. Reddy SS, Upreti KK, Burondkar MM,

699   Bhagwan A, Kennedy R. 2011. Application of extended BBCH Scale for phenological

700   studies in mango (*Mangifera indica* L.). Journal of Applied Horticulture 13:108–114.

701   DOI: 10.37855/jah.2011.v13i02.25.

702   Ramírez F, Davenport TL. 2010. Mango (*Mangifera indica* L.) flowering physiology. Scientia

703   Horticulturae 126:65–72. DOI: 10.1016/j.scienta.2010.06.024.

704   Ramírez F, Davenport TL, Fischer G, Pinzón JCA, Ulrichs C. 2014. Mango trees have no

705   distinct phenology: The case of mangoes in the tropics. Scientia Horticulturae 168:258–

706   266. DOI: 10.1016/j.scienta.2014.01.040.

707   Samach A, Onouchi H, Gold SE, Ditta GS, Schwarz-Sommer Z, Yanofsky MF, Coupland G.

708   2000. Distinct Roles of *CONSTANS* Target Genes in Reproductive Development of

709   Arabidopsis. Science 288:1613–1616. DOI: 10.1126/science.288.5471.1613.

710   dos Santos Silva L, de Sousa KÂO, Pereira ECV, Rolim LA, da Cunha JG, Santos MC, da Silva

711   MA, Cavalcante ÍHL. 2021. Advances in mango 'Keitt' production system: PBZ

712   interaction with fulvic acids and free amino acids. Scientia Horticulturae 277:109787.

713   DOI: 10.1016/j.scienta.2020.109787.

714   de los Santos-Villalobos S, de Folter S, Délano-Frier JP, Gómez-Lim MA, Guzmán-Ortiz DA,

715   Peña-Cabriales JJ. 2013. Growth Promotion and Flowering Induction in Mango

716   (*Mangifera indica* L. cv "Ataulfo") Trees by Burkholderia and Rhizobium Inoculation:

717   Morphometric, Biochemical, and Molecular Events. Journal of Plant Growth Regulation

718   32:615–627. DOI: 10.1007/s00344-013-9329-5.

719   Schwacke R, Grallath S, Breitkreuz KE, Stransky E, Stransky H, Frommer WB, Rentsch D.

720   1999. LeProT1, a Transporter for Proline, Glycine Betaine, and γ-Amino Butyric Acid in

721   Tomato Pollen. The Plant Cell 11:377–391. DOI: 10.1105/tpc.11.3.377.

722   Seif El-Yazal MA, Seif El-Yazal SA, Rady MM. 2014. Exogenous dormancy-breaking

723   substances positively change endogenous phytohormones and amino acids during

724   dormancy release in 'Anna' apple trees. Plant Growth Regulation 72:211–220. DOI:

725   10.1007/s10725-013-9852-1.

726   Sellmer J, Adkins CR, McCall I, Whipker B. 1999. 258 Pampas Grass (Cortaderia argentea)

727   Response to Ancymidol, Paclobutrazol, and Uniconazole Substrate Drenches.

728   HortScience 34:486E – 486. DOI: 10.21273/HORTSCI.34.3.486E.

729   Sharma D, Awasthi MD. 2005. Uptake of soil applied paclobutrazol in mango (*Mangifera indica*

730   L.) and its persistence in fruit and soil. Chemosphere 60:164–169. DOI:

731   10.1016/j.chemosphere.2004.12.069.

732   Shivashankara KS, Geetha GA, Roy and TK. 2019. Influence of girdling on flower sex ratio,

733   biochemical constituents, and fruit set intensity in mango (*Mangifera indica* L.). Biologia

734   plantarum 63:432–439. DOI: 10.32615/bp.2019.064.

735   Silva PT de S e, Souza LS da S, Neta CR, Mouco MA, Simoes W, Ferraz A. 2017. Análise de

736   paclobrutrazol em solos de áreas cultivadas com diferentes variedades de mangueira no

737   Vale do São Francisco empregando QuEcHers e CLAE. Scientia Plena 13. DOI:

738   10.14808/sci.plena.2017.097201.

739 Singh VK, Bhattacherjee AK. 2005. Genotypic response of mango yield to persistence of

740   paclobutrazol in soil. Scientia Horticulturae 106:53–59. DOI:

741   10.1016/j.scienta.2005.02.012.

742 Sreeharsha RV, Mudalkar S, Singha KT, Reddy AR. 2016. Unravelling molecular mechanisms

743   from floral initiation to lipid biosynthesis in a promising biofuel tree species, Pongamia

744   pinnata using transcriptome analysis. Scientific Reports 6:34315. DOI:

745   10.1038/srep34315.

746 Srilatha V, Reddy YTN. 2015. Pruning and Paclobutrazol Induced Flowering and Changes in

747   Phenols and Flavonoids of Mango (*Mangifera indica* L.) cv. Raspuri. Applied Sciences

748   4:5.

749 Srilatha V, Reddy YTN, Upreti KK, Venugopalan R, Jayaram HL. 2016. Responses of pruning

750   and paclobutrazol in mango (*Mangifera indica* L.): changes in tree vigour, flowering and

751   phenols. Journal of Applied Horticulture 18:148–153. DOI:

752   10.37855/jah.2016.v18i02.26.

753 Stonehouse JM. 2001. An overview of fruit fly research knowledge and needs in the Indian

754   Ocean region. In: Proceedings of the second national symposium on integrated pest

755   management (IPM) in horticultural crops: new molecules, biopesticides and environment.

756   In: Bangalore,.

757 Thévenot EA, Roux A, Xu Y, Ezan E, Junot C. 2015. Analysis of the Human Adult Urinary

758   Metabolome Variations with Age, Body Mass Index, and Gender by Implementing a

759   Comprehensive Workflow for Univariate and OPLS Statistical Analyses. Journal of

760   Proteome Research 14:3322–3335. DOI: 10.1021/acs.jproteome.5b00354.

761   Tiwari DK, Patel V, Pandey A. 2018. Floral induction in mango: Physiological, biochemical and

762   molecular basis. International Journal of Chemical Studies 6:252–259.

763   Upreti KK, Reddy YTN, Prasad SRS, Bindu GV, Jayaram HL, Rajan S. 2013. Hormonal

764   changes in response to paclobutrazol induced early flowering in mango cv. Totapuri.

765   Scientia Horticulturae 150:414–418. DOI: 10.1016/j.scienta.2012.11.030.

766   Upreti KK, Shivu Prasad SR, Reddy YTN, Rajeshwara AN. 2014. Paclobutrazol induced

767   changes in carbohydrates and some associated enzymes during floral initiation in mango

768   (*Mangifera indica* L.) cv. Totapuri. Indian Journal of Plant Physiology 19:317–323. DOI:

769   10.1007/s40502-014-0113-8.

770   Wang H, Hua J, Yu Q, Li J, Wang J, Deng Y, Yuan H, Jiang Y. 2021. Widely targeted

771   metabolomic analysis reveals dynamic changes in non-volatile and volatile metabolites

772   during green tea processing. Food Chemistry 363:130131. DOI:

773   10.1016/j.foodchem.2021.130131.

774   Wang D, Liu XX, Li TT, Li Q, Liu Y, Gong GS, Yang H. 2018a. First Report of Cucumber

775   mosaic virus Infection in Kiwifruit (*Actinidia chinensis*) in China. Plant Disease

776   102:1180–1180. DOI: 10.1094/PDIS-06-17-0824-PDN.

777   Wang D, Zhang L, Huang X, Wang X, Yang R, Mao J, Wang X, Wang X, Zhang Q, Li P.

778   2018b. Identification of Nutritional Components in Black Sesame Determined by Widely

779   Targeted Metabolomics and Traditional Chinese Medicines. Molecules 23:1180. DOI:

780   10.3390/molecules23051180.

781   Wilkie JD, Sedgley M, Olesen T. 2008. Regulation of floral initiation in horticultural trees.

782   Journal of Experimental Botany 59:3215–3228. DOI: 10.1093/jxb/ern188.

783   Wu Q, Du M, Wu J, Wang N, Wang B, Li F, Tian X, Li Z. 2019. Mepiquat chloride promotes

784   cotton lateral root formation by modulating plant hormone homeostasis. BMC Plant

785   Biology 19:1–16. DOI: 10.1186/s12870-019-2176-1.

786   Xiao J, Gu C, He S, Zhu D, Huang Y, Zhou Q. 2021. Widely targeted metabolomics analysis

787   reveals new biomarkers and mechanistic insights on chestnut (*Castanea mollissima* Bl.)

788   calcification process. Food Research International 141:110128. DOI:

789   10.1016/j.foodres.2021.110128.

790   Xing D, Feng W, Nöt LG, Miller AP, Zhang Y, Chen Y-F, Majid-Hassan E, Chatham JC, Oparil

791   S. 2008. Increased protein *O -GlcNAc* modification inhibits inflammatory and neointimal

792   responses to acute endoluminal arterial injury. American Journal of Physiology-Heart and

793   Circulatory Physiology 295:H335–H342. DOI: 10.1152/ajpheart.01259.2007.

794   Xing L-B, Zhang D, Li Y-M, Shen Y-W, Zhao C-P, Ma J-J, An N, Han M-Y. 2015.

795   Transcription Profiles Reveal Sugar and Hormone Signaling Pathways Mediating Flower

796   Induction in Apple (*Malus domestica Borkh*.). Plant and Cell Physiology 56:2052–2068.

797   DOI: 10.1093/pcp/pcv124.

798   Yan X, Liu J, Wu K-X, Yang N, Pan L-B, Song Y, Liu Y, Tang Z-H. 2022. Comparative

799   Analysis of Endogenous Hormones and Metabolite Profiles in Early-Spring Flowering

800   Plants and Unflowered Plants Revealing the Strategy of Blossom. Journal of Plant

801   Growth Regulation 41:2421–2434. DOI: 10.1007/s00344-021-10452-w.

802   Yang Q, Gao Y, Wu X, Moriguchi T, Bai S, Teng Y. 2021. Bud endodormancy in deciduous

803   fruit trees: advances and prospects. Horticulture Research 8:139. DOI: 10.1038/s41438-

804   021-00575-2.

805   Yi D, Zhang H, Lai B, Liu L, Pan X, Ma Z, Wang Y, Xie J, Shi S, Wei Y. 2021. Integrative

806   Analysis of the Coloring Mechanism of Red Longan Pericarp through Metabolome and

807   Transcriptome Analyses. Journal of Agricultural and Food Chemistry 69:1806–1815.

808   DOI: 10.1021/acs.jafc.0c05023.

809   Zhang H, Li H, Lai B, Xia H, Wang H, Huang X. 2016. Morphological Characterization and

810   Gene Expression Profiling during Bud Development in a Tropical Perennial, Litchi

811   chinensis Sonn. Frontiers in Plant Science 7. DOI: 10.3389/fpls.2016.01517.

812   Zhang W, Li J, Zhang W, Njie A, Pan X. 2022. The changes in C/N, carbohydrate, and amino

813   acid content in leaves during female flower bud differentiation of Juglans sigillata. Acta

814   Physiologiae Plantarum 44:19. DOI: 10.1007/s11738-021-03328-9.

815   Zhang J, Qiu X, Tan Q, Xiao Q, Mei S. 2020. A Comparative Metabolomics Study of Flavonoids

816   in Radish with Different Skin and Flesh Colors (*Raphanus sativus* L .). Journal of

817   Agricultural and Food Chemistry 68:14463–14470. DOI: 10.1021/acs.jafc.0c05031.

818   Zheng B, Zhao Q, Wu H, Wang S, Zou M. 2021. A Comparative Metabolomics Analysis of

819   Guava (*Psidium guajava* L.) Fruit with Different Colors. ACS Food Science &

820   Technology 1:96–106. DOI: 10.1021/acsfoodscitech.0c00036.

821   Zhou X, Liu Y, Huang J, Liu Q, Sun J, Cai X, Tang P, Liu W, Miao W. 2019. High temperatures

822   affect the hypersensitive reaction, disease resistance and gene expression induced by a

823   novel harpin HpaG-Xcm. Scientific Reports 9:990. DOI: 10.1038/s41598-018-37886-9.

824   Zhuang W, Gao Z, Wang L, Zhong W, Ni Z, Zhang Z. 2013. Comparative proteomic and

825   transcriptomic approaches to address the active role of GA4 in Japanese apricot flower

826   bud dormancy release. Journal of Experimental Botany 64:4953–4966. DOI:

827   10.1093/jxb/ert284.

828   Zhuang W, Gao Z, Wen L, Huo X, Cai B, Zhang Z. 2015. Metabolic changes upon flower bud

829   break in Japanese apricot are enhanced by exogenous GA4. Horticulture Research

830   2:15046. DOI: 10.1038/hortres.2015.46.

831   Zou S, Wu J, Shahid MQ, He Y, Lin S, Liu Z, Yang X. 2020. Identification of key taste

832   components in loquat using widely targeted metabolomics. Food Chemistry 323:126822.

833   DOI: 10.1016/j.foodchem.2020.126822.

834

Figure 1

Figure 1 Morphological changes of mango buds at different stages of floral induction and initiation.

TA, TB, TC, A, B and C indicates sample names. T-30/C-30 indicates mango stem apex at 30 days after SPD/water treatment.T-60/C-60 indicates mango stem apex at 60 days after SPD/water treatment.T-80/C-80 indicates mango stem apex at 80 days after SPD/water treatment.T-100/C-100 indicates mango stem apex at 100 days after SPD/water treatment.T-120/C-120 indicates mango stem apex at 120 days after SPD/water treatment.
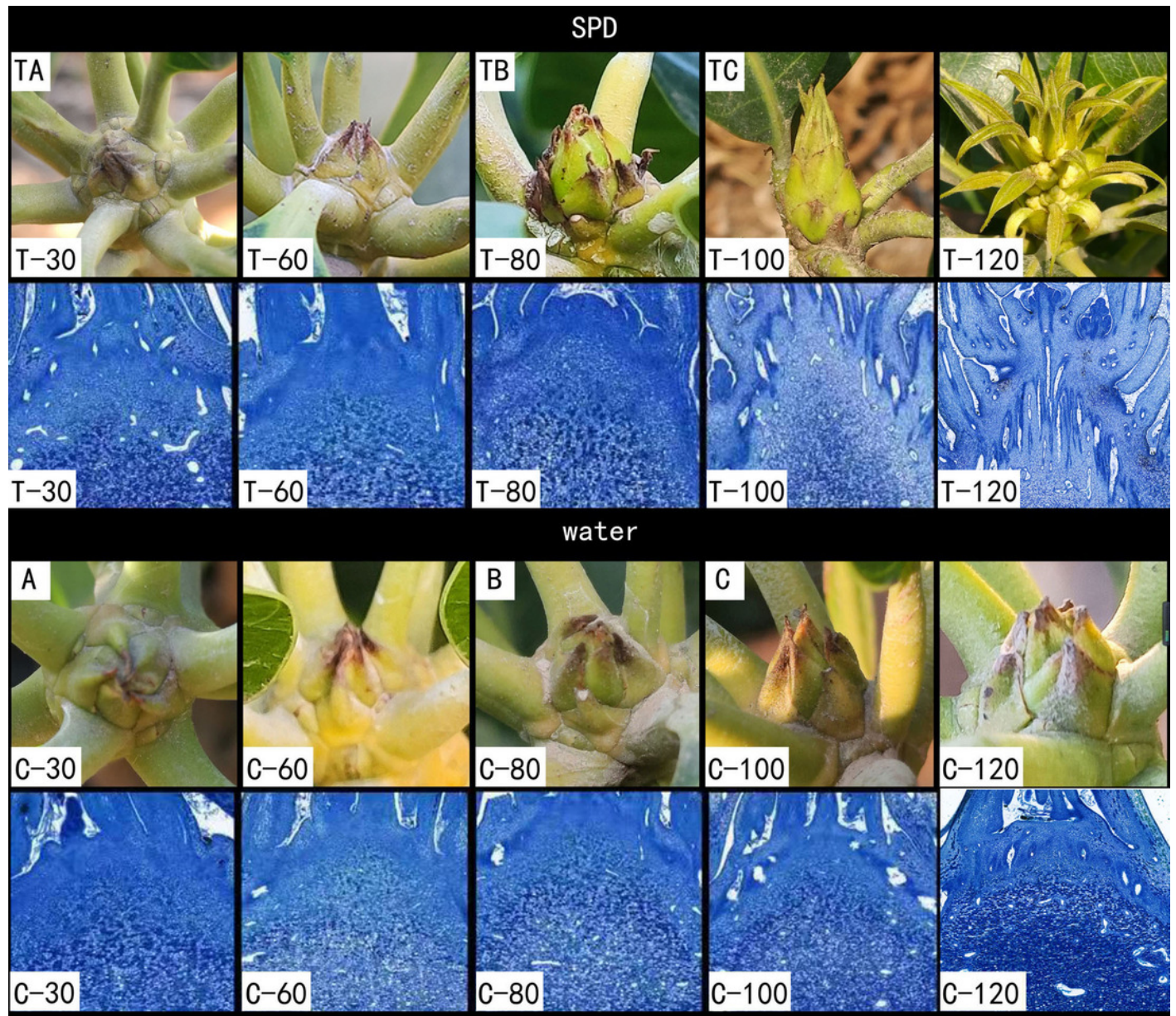
Figure 2

Figure 2 Flowering rate and yield per tree were after SPD treatment or water (Control) in 2020 and 2021.

(A) Flowering rate; (B) Mango yield per tree. Note: * indicates statistical significance with $p < 0.05$, ** indicates statistical significance with $p < 0.01$, *** indicates statistical significance with $p < 0.001$. The numbers in figure represent the number of mango.
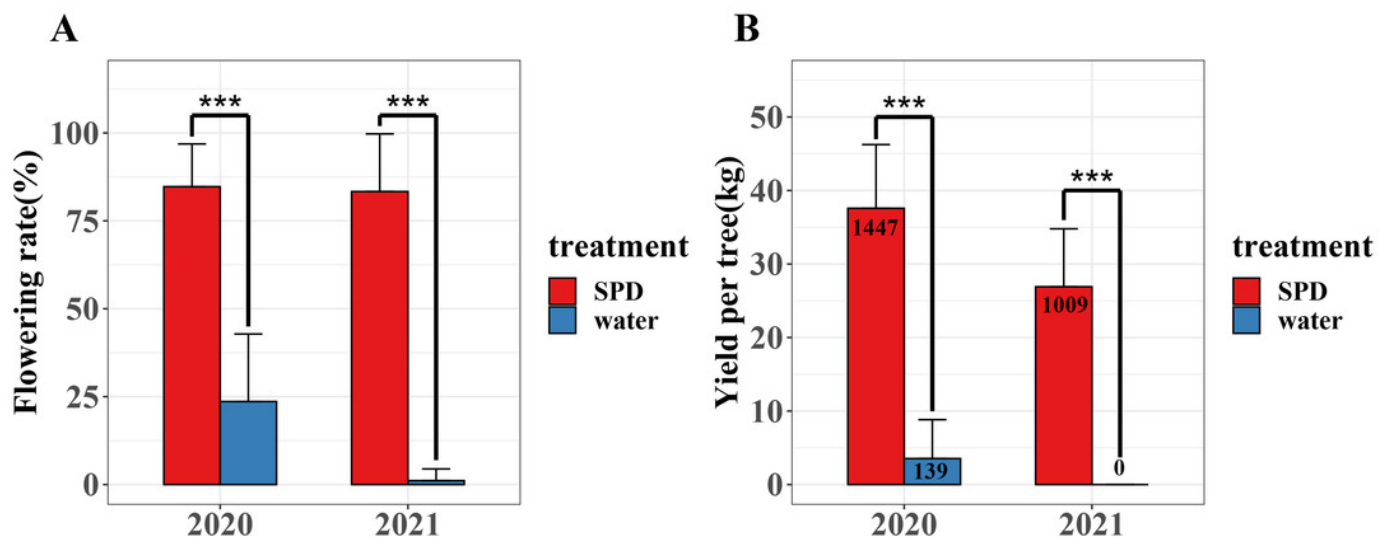
Figure 3

Figure 3 Metabolic characteristics of buds at different days.

(A) Principal component analysis of metabolites TA, TB, TC, A, B and C. PC1 represents the first principal component, PC2 represents the second principal component, and the percentage represents the interpretation rate of the principal component of the data set. Each dot in the diagram represents a sample, and samples from the same group are represented in the same color; TA-1, TA-2 and TA-3 are three repetitions of TA. TB-1, TB-2 and TB-3 are three repetitions of TB. TC-1, TC-2 and TC-3 are three repetitions of TC. A-1, A-2 and A-3 are three repetitions of A. B-1, B-2 and B-3 are three repetitions of B. C-1, C-2 and C-3 are three repetitions of C. QC-1, QC-2 and QC-3 are three repetitions of QC. (B) Sample correlation analysis of mango buds during FI based on relative amounts of metabolite contents. stem apex in three stages (treated with SPD/water), the abscissa and ordinate represent the sample name, and the color represents the correlation value (red represents high, green represents low). (C) Hierarchical cluster analysis of metabolites from samples of TA, TB, TC, A, B and C. The horizontal represents the metabolites, the vertical represents the sample name, and the different colors are the values obtained by standardization of the relative amounts (red represents high, blue represents low).
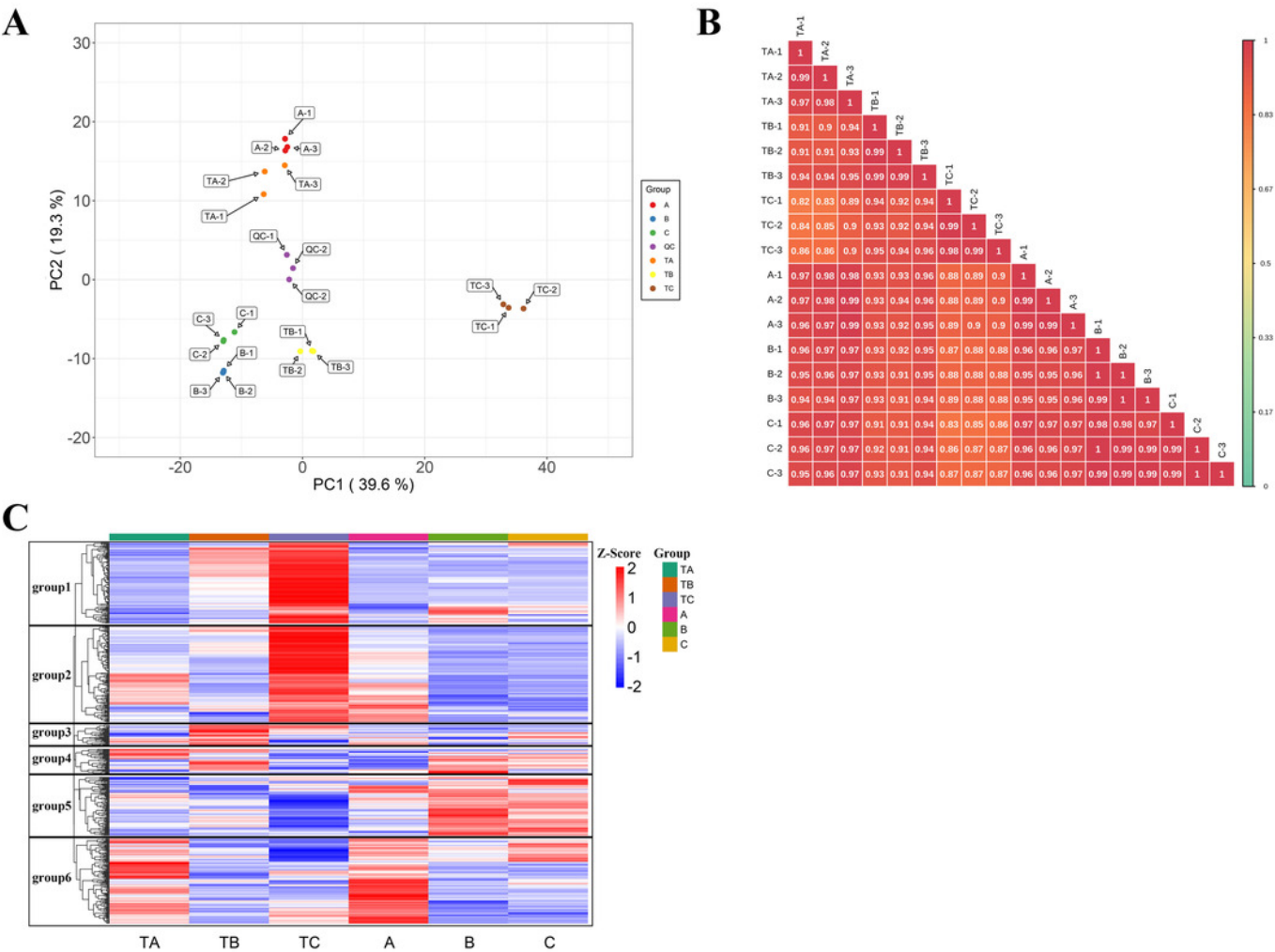
Figure 4

Figure 4 Differential metabolites between different groups.

(A) Differential metabolites between different sample. The abscissa indicates the quantity of differential metabolites, the ordinate indicates different groups, and red represent up-regulated differential metabolites, and blue represent down-regulated differential metabolites. And up regulated / down regulated is the change of the former relative to the latter. (B) Venn diagram of differential metabolites B vs A, C vs A, and C vs B. (C) Venn diagram of differential metabolites TB vs TA, TC vs TA, and TC vs TB. (D) Venn diagram of differential metabolites TA vs A, TB vs B, and TC vs C.

A
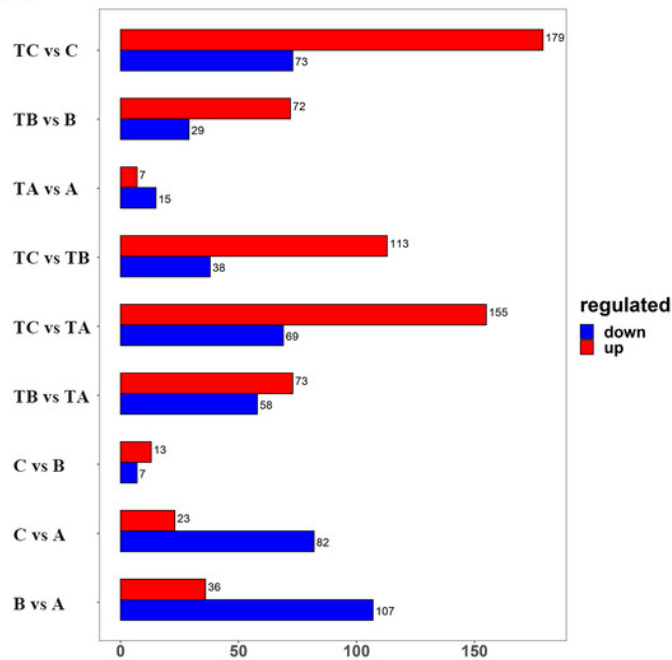
B
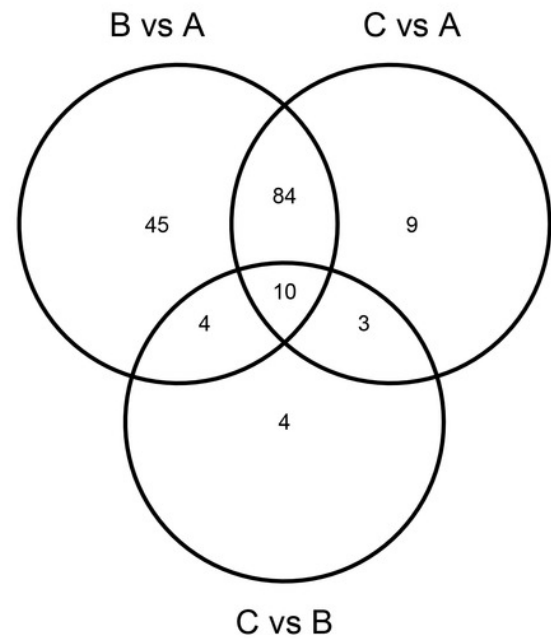
C
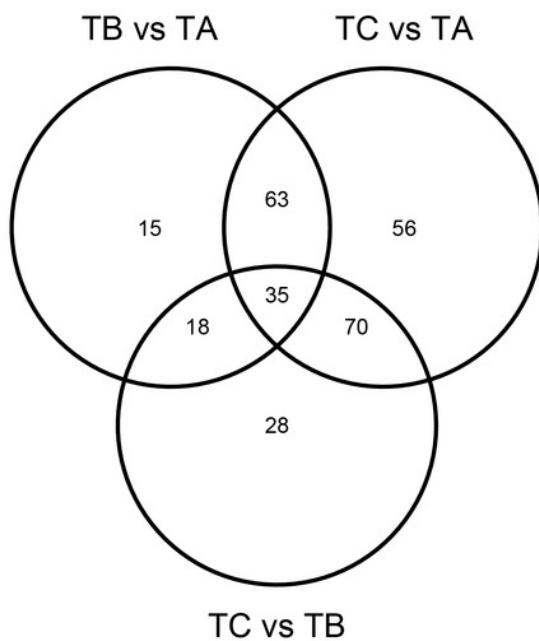
D
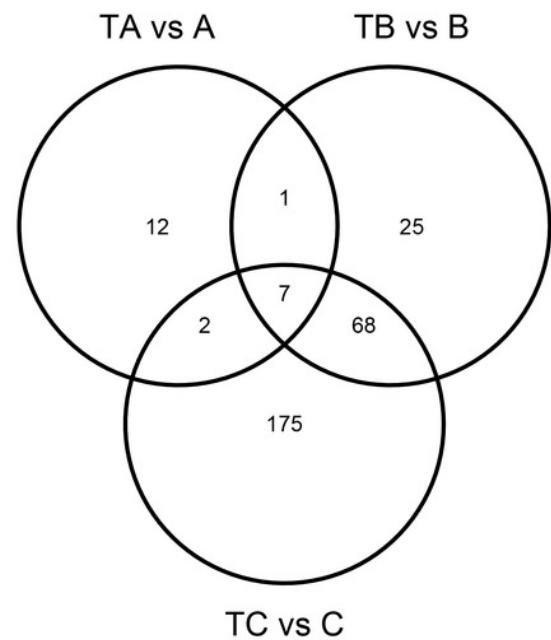
Figure 5

Figure 5 KEGG enrichment analysis of differential metabolites.

(A) TA vs A, (B) TB vs B, and (C) TC vs C; The abscissa indicates the Rich factor corresponding to each channel, the ordinate indicates the channel name, and the color of the point is P value. The redder indicates that the enrichment is more significant. The size of the dot represents the number of enriched differential metabolites.
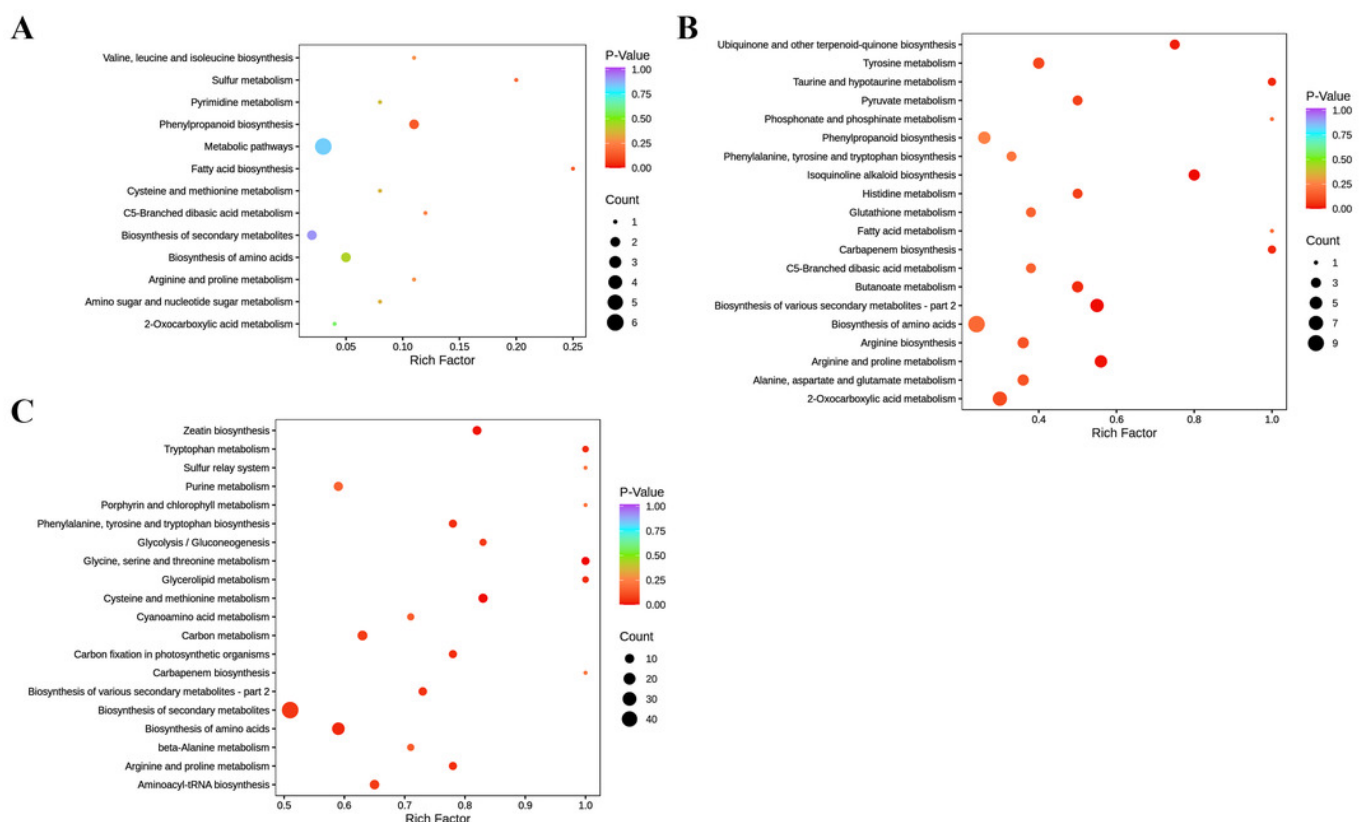
Figure 6

Figure 6 K-means analysis of all differential metabolites.

Abscissa indicates the name of the sample, ordinate indicates the standardized relative amounts of metabolites, and the numeric characters following each cluster indicates the number of metabolites in this cluster.
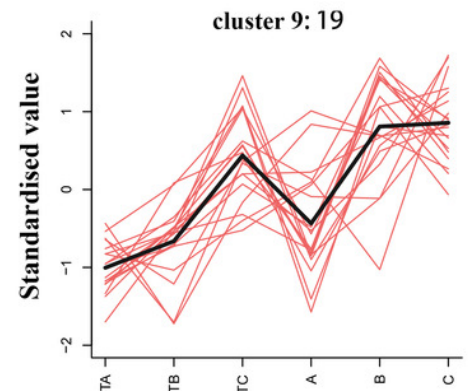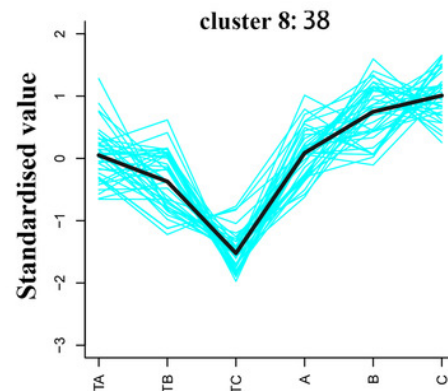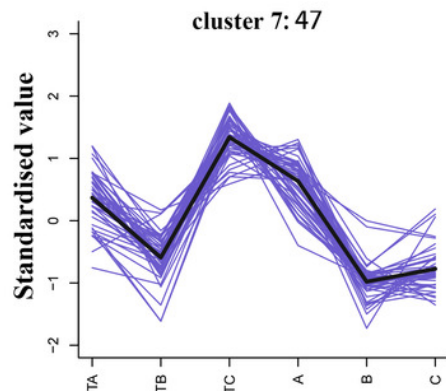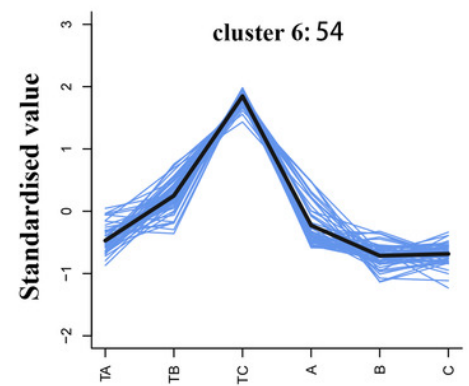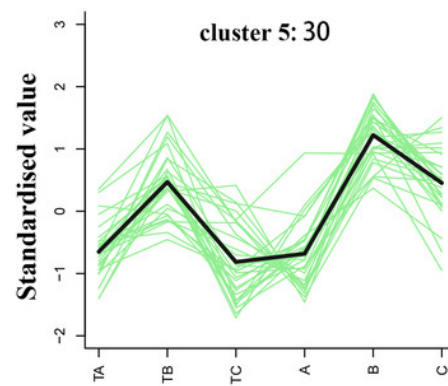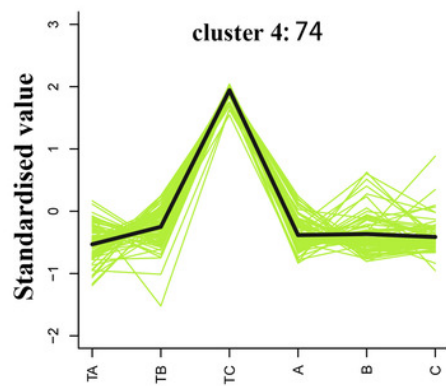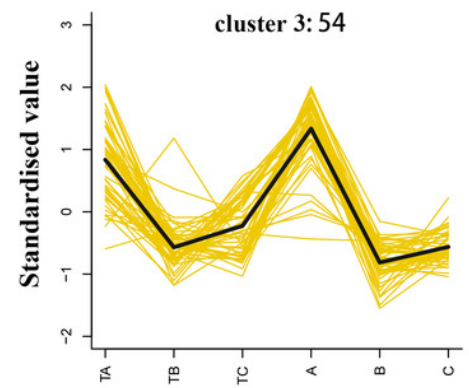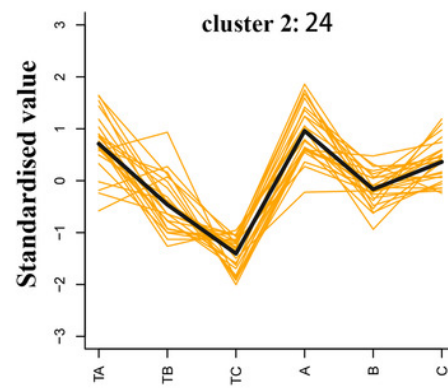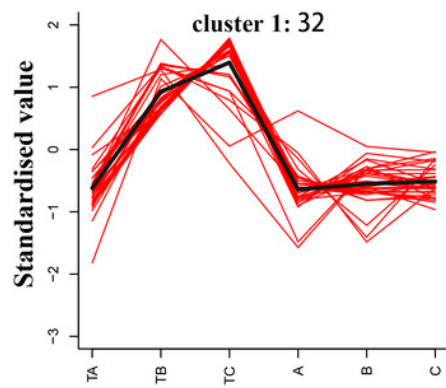
Figure 7

Figure 7 Heat map of differential metabolite contents in the mango stem apex at different stages.

(A) Heat map of amounts of 53 differential metabolite content at three stages of FI (TA, TB, and TC); (B) Levels of metabolites in proline biosynthesis pathway in mango stem apex at three stages of Fl. (C) Heat map of amounts of 18 differential metabolite (7 vitamins and 11 saccharides and alcohols) content at three stages of FI (TA, TB, TC, A, B and C); Note: heat map shows the level of metabolites in mango terminal buds at three stages, and blue to red in heat map shows the level of metabolites from low to high.
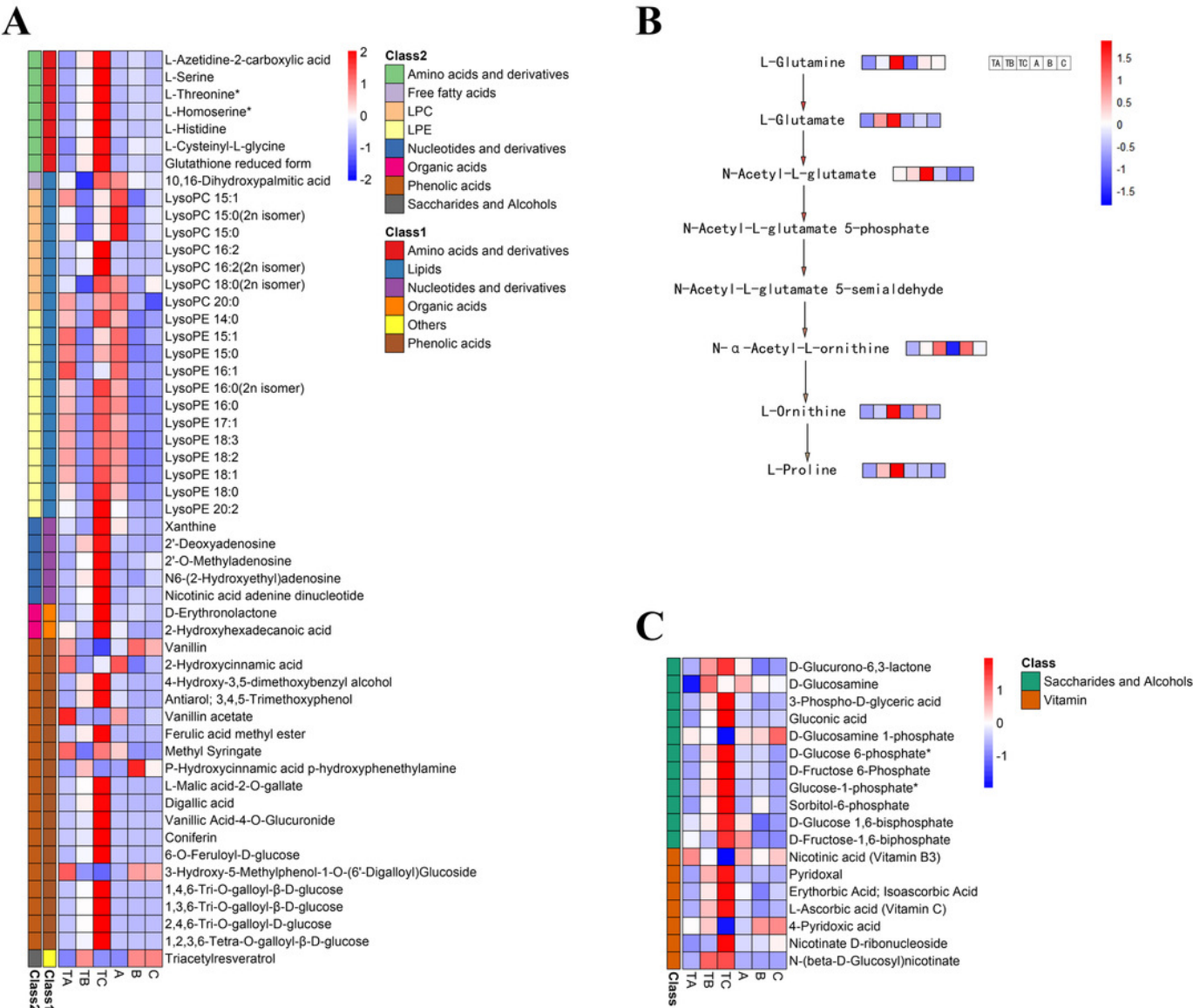
Figure 8

Figure 8 Metabolites with relative abundance changed more than 10 times.

The abscissa is group, the ordinate is differential metabolites, and the numbers in the diagram relate to logarithmic value of differential multiples of differential metabolites based on 2.

A vs B	A vs C	B vs C	TA vs TB	TA vs TC	TB vs TC	
0.30	0.56	0.26	9.98	10.68	0.70	L-Homocysteine
-0.15	0.05	0.19	1.61	3.37	1.76	L-Histidine
-0.34	-0.16	0.17	0.47	4.57	4.09	L-Homomethionine
-0.41	-0.19	0.22	1.70	3.48	1.78	Digallic acid
-0.25	-0.62	-0.36	3.52	6.74	3.22	Vanillic Acid-4-O-Glucuronide
-0.34	0.09	0.42	4.86	3.98	-0.88	1-O-Galloyl-2-O-Cinnamoyl-β-D-glucose
-1.13	0.05	1.19	4.64	5.39	0.75	2,3-Di-O-Galloyl-D-Glucose
-0.77	-0.05	0.72	1.59	3.74	2.14	LysoPC 16:2
-0.75	-0.12	0.63	1.58	3.93	2.35	LysoPC 16:2(2n isomer)
-0.12	-0.21	-0.10	2.29	4.53	2.24	1,4,6-Tri-O-galloyl-β-D-glucose
0.03	-0.02	-0.05	2.84	5.02	2.17	1,3,6-Tri-O-galloyl-β-D-glucose
-0.47	0.12	0.60	2.51	4.59	2.08	2,4,6-Tri-O-galloyl-D-glucose
0.90	0.76	-0.15	1.80	3.57	1.76	Nicotinic acid adenine dinucleotide
-0.05	-0.07	-0.01	1.82	4.18	2.36	1,2,3,6-Tetra-O-galloyl-β-D-glucose

Legend: 10, 8, 6, 4, 2, 0